Acta Crystallographica Section B
Structural Science
ISSN 0108-7681

Symmetry rules and strain/order-parameter relationships for coupling between octahedral tilting and cooperative Jahn–Teller transitions in ABX_3 perovskites. I. Theory

Michael A. Carpenter[a]* and Christopher J. Howard[a,b]

[a]Department of Earth Sciences, University of Cambridge, Downing Street, Cambridge CB2 3EQ, England, and [b]School of Engineering, University of Newcastle, NSW 2308, Australia

Correspondence e-mail: mc43@esc.cam.ac.uk

Received 17 October 2008
Accepted 8 January 2009

Space groups, order-parameter and strain/order-parameter coupling relationships in ABX_3 perovskite structures which combine cooperative Jahn–Teller distortions and octahedral tilting have been investigated from the perspective of group theory using the computer program *ISOTROPY*. Two common Jahn–Teller ordering schemes are associated with the irreducible representations M_2^+ and R_3^+ of the space group $Pm\bar{3}m$. A third, less-common ordering scheme is associated with Γ_3^+. These combine with tilting instabilities associated with M_3^+ and R_4^+ to generate a predicted suite of Jahn–Teller structure types that includes many of the known structures of manganites, vanadates, Cu and Cr halides. Order-parameter coupling and possible phase transitions are described using Landau free-energy expansions, and general expressions for the relationships between symmetry-adapted spontaneous strains and particular order-parameter components are presented. These provide a general formal framework for determining structural evolution across multi-component order-parameter space and for characterizing the influence of tilting instabilities on Jahn–Teller instabilities or of Jahn–Teller ordering on octahedral tilting.

1. Introduction

A characteristic feature of the wide array of phase transitions which occur in perovskites as a response to changes in temperature and pressure is that they can be driven by multiple instabilities, even in a sample with simple, fixed stoichiometry. Different combinations of displacive, cation-ordering and electronic transitions give rise to the familiar diversity of ferroelastic, ferroelectric, magnetic and electrical properties which continue to attract intense interest from both scientific and technological perspectives. Composition can also be adjusted across multicomponent solid solutions to substantially increase the phenomenological richness of these materials as single crystals, powders, ceramics or thin films. An important subgroup of multiple combinations of phase transitions in perovskites involves octahedral tilting and cooperative Jahn–Teller distortions. Although restricted to phases containing the relatively small number of cations with uneven occupation of t_{2g} or, more notably, e_g orbitals by d electrons, including Ti^{3+}, V^{3+}, Cr^{2+}, Mn^{3+}, Fe^{2+}, Co^{2+}, Co^{3+}, Ni^{3+} and Cu^{2+} in high-spin states, Fe^{3+} and Co^{4+} in low-spin states, and Fe^{2+}, Fe^{3+}, Co^{3+} and Co^{4+} in intermediate spin states, the Jahn–Teller effect has a special significance because it links changes in electronic configuration to changes in structural state (*e.g.* Goodenough, 1998, 2004; Salamon & Jaime, 2001; Israel *et al.*, 2007; and many references therein). Since octahedral tilting and Jahn–Teller distortions influence each other (*e.g.* Mizokawa *et al.*, 1999), a link necessarily also exists between tilting

transitions and electronic properties. Landau theory and group-theoretical rules provide a rigorous basis for determining the form and character of allowed interactions between different structural instabilities, and the first aim of the present work was to set out space group and order-parameter relationships for different combinations of cooperative Jahn–Teller distortions with M-point + R-point tilting in ABX_3 perovskites. As well as providing a proper basis for rationalizing known structure types and the phase transitions which occur between them, this approach allows the prediction of other order-parameter combinations and structure types which have not yet been observed.

Geometrical aspects of Jahn–Teller distortions, cation ordering and octahedral tilting have recently been reviewed by Lufaso & Woodward (2004) and Tamazyan & van Smaalen (2007). Group–subgroup symmetry relations for some of the structures have also been considered by Bock & Müller (2002). The Jahn–Teller distortion of an individual BX_6 octahedron is associated with breaking of the degeneracy of the d-electron orbitals of the B cation, and the form of the distortion is commonly labelled Q_2 or Q_3 (Goodenough, 1998, 2004). If two $B-X$ bonds lengthen and two contract (Q_2), the cubic geometry of a regular octahedron becomes orthorhombic. If two bonds lengthen (or contract) and the remaining four contract (or lengthen; Q_3) the point symmetry becomes tetragonal. Ordered arrangements of orbital occupancies are then manifest as ordered arrangements of distorted octahedra.

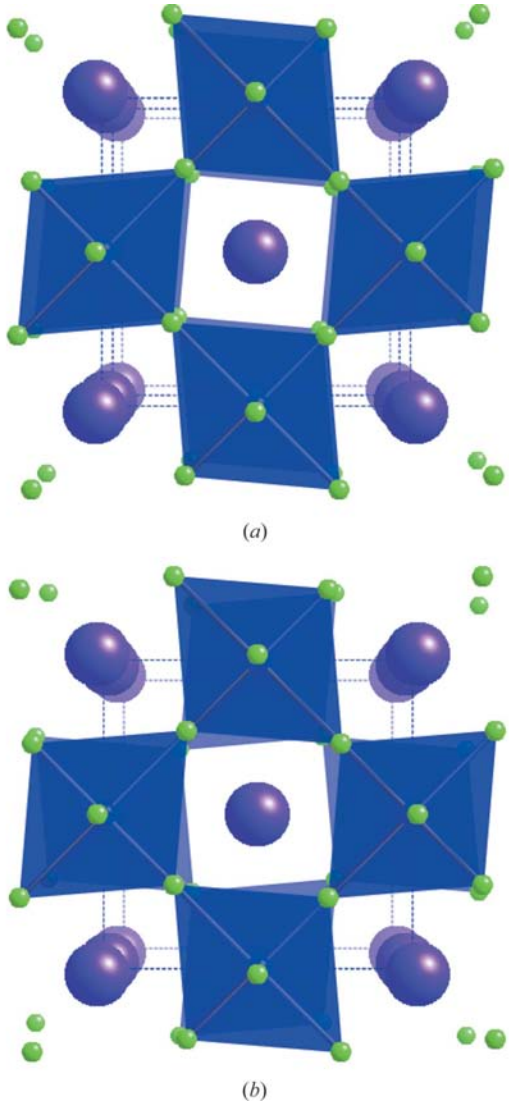

Figure 1
Polyhedral representations of the structural variants of the Jahn–Teller distorted perovskite $KCuF_3$. (*a*) Variant with space-group symmetry *P*4/*mbm*, known as *d*-type or *C*-type; the distortion is associated with irrep M_2^+. (*b*) Variant with space-group symmetry *I*4/*mcm*, known as *a*-type or *G*-type, the irrep here being R_3^+.

Two of the key Jahn–Teller ordering schemes in perovskites are well understood from structures of $KCuF_3$, which do not undergo octahedral tilting. Both contain planes of octahedra within which long and short Cu—F bonds alternate. In the structure with space group *P*4/*mbm*, these planes are stacked one directly above the other (Fig. 1*a*). This structure has been referred to as *d*-type (Okazaki, 1969*a*,*b*; Lufaso & Woodward, 2004) or sometimes as *C*-type (Sage *et al.*, 2007), by analogy with the notation used in the description of antiferromagnetic structures (Wollan & Koehler, 1955). The structure in which alternate planes are rotated so that the long Cu—F bond in one plane lies directly above the short bond in the next (Fig. 1*b*), with the space group *I*4/*mcm*, is labelled *a*-type (Okazaki, 1969*a*) or *G*-type (Sage *et al.*, 2007). In both structures, the distortions of individual octahedra are Q_2 according to the atomic displacements associated with the symmetry change from the parent cubic form ($Pm\bar{3}m$), but the symmetry is also permissive of Q_3. A third possibility has the unique tetragonal axes of Q_3 octahedra all aligned in the same direction. An example of this structure appears to be the form of $La_{0.5}Ba_{0.5}CoO_3$ which has disordered cations on the A sites and a reported space group of *P*4/*mmm* (Fauth *et al.*, 2001).

Superposition of octahedral tilting on *d*- and *a*-type ordering schemes gives the well known structures, for example, of $LaMnO_3$ and related manganites (*e.g.* Norby *et al.*, 1995; Huang *et al.*, 1997; Rodríguez-Carvajal *et al.*, 1998; Alonso *et al.*, 2000; Tachibana *et al.*, 2007), YVO_3 and related vanadates (*e.g.* Bordet *et al.*, 1993; Blake *et al.*, 2001, 2002; Ren *et al.*, 2003; Sage *et al.*, 2007; Martínez-Lope *et al.*, 2008), $LaTiO_3$ and related titanites (*e.g.* Mizokawa *et al.*, 1999; Hemberger *et al.*, 2003; Komarek *et al.*, 2007). Given the large number of M-point, R-point and $M + R$ point tilt systems, however (Glazer, 1972; Woodward, 1997*a*,*b*; Howard & Stokes, 1998), there should exist a significant number of possible mixed tilting + orbitally ordered structures. Not all combinations will necessarily be allowed by symmetry and those that are may not be easy to recognize purely by their lattice geometry, hence the need for the present group-theoretical treatment.

An additional theme which permeates attempts to understand the structure and properties of real Jahn–Teller perovskites, such as the manganites and vanadates, is the importance of strain (*e.g.* Millis, 1998; Millis *et al.* 1998; Uehara & Cheong, 2000; Ahn & Millis, 2001; Podzorov *et al.*, 2001; Gu & Ting, 2002; Miyasaka *et al.*, 2003; Sánchez *et al.*, 2003;

Table 1
Space groups, order-parameter components, tilt systems and unit-cell relationships for ABX_3 perovskites containing octahedral tilting related to irreps M_3^+ and/or R_4^+ together with ordered arrangements of Jahn–Teller distorted octahedra related to irreps Γ_3^+, M_2^+ or R_3^+.

The lattice vectors and origins are given for conventional settings of the space groups, in the manner described by Howard & Stokes (1998). When both JT distortions and octahedral tilting are present, the same orientations of tilt axes with respect to reference axes *X*, *Y* and *Z* as occur for tilting only have been preserved. In mixed structures, the different possible orientations of the JT ordering schemes with respect to the reference axes have been considered, as these can lead to more than one structure type for a given tilt system.

	Space group		M_3^+ $q_1q_2q_3$	R_4^+ $q_4q_5q_6$	System	Lattice vectors	Origin
1	221 $Pm\bar{3}m$		(0,0,0)	(0,0,0)	$a^0a^0a^0$	(1,0,0)(0,1,0)(0,0,1)	(0,0,0)
2	127 $P4/mbm$		(a,0,0)	(0,0,0)	$a^0a^0c^+$	(1,1,0)($\bar{1}$,1,0)(0,0,1)	(0,0,0)
3	139 $I4/mmm$		(a,0,a)	(0,0,0)	$a^0b^+b^+$	(0,2,0)(0,0,2)(2,0,0)	($\frac{1}{2}$,$\frac{1}{2}$,$\frac{3}{2}$)
4	204 $Im\bar{3}$		(a,a,a)	(0,0,0)	$a^+a^+a^+$	(2,0,0)(0,2,0)(0,0,2)	($\frac{1}{2}$,$\frac{1}{2}$,$\frac{1}{2}$)
5	71 $Immm$		(a,b,c)	(0,0,0)	$a^+b^+c^+$	(2,0,0)(0,2,0)(0,0,2)	($\frac{1}{2}$,$\frac{1}{2}$,$\frac{1}{2}$)
6	140 $I4/mcm$		(0,0,0)	(a,0,0)	$a^0a^0c^-$	(1,1,0)($\bar{1}$,1,0)(0,0,2)	(0,0,0)
7	74 $Imma$		(0,0,0)	(a,0,a)	$a^0b^-b^-$	(0,1,1)(2,0,0)(0,1,$\bar{1}$)	(0,0,0)
8	167 $R\bar{3}c$		(0,0,0)	(a,a,a)	$a^-a^-a^-$	($\bar{1}$,1,0)(0,$\bar{1}$,1)(2,2,2)	(0,0,0)
9	12 $C2/m$		(0,0,0)	(a,0,b)	$a^0b^-c^-$	(0,$\bar{2}$,0)(2,0,0)(0,1,1)	($\frac{1}{2}$,$\frac{1}{2}$,0)
10	15 $C2/c$		(0,0,0)	(a,b,a)	$a^-b^-b^-$	(2,$\bar{1}$,$\bar{1}$)(0,1,$\bar{1}$)(0,1,1)	($\frac{1}{2}$,$\frac{1}{2}$,0)
11	2 $P\bar{1}$		(0,0,0)	(a,b,c)	$a^-b^-c^-$	(0,1,1)(1,0,1)(1,1,0)	(0,0,0)
12	63 $Cmcm$		(0,0,a)	(b,0,0)	$a^0b^+c^-$	(2,0,0)(0,0,$\bar{2}$)(0,2,0)	($\frac{1}{2}$,0,$\frac{1}{2}$)
13	62 $Pnma$		(0,a,0)	(b,0,b)	$a^+b^-b^-$	(0,1,1)(2,0,0)(0,1,$\bar{1}$)	(0,0,0)
14	11 $P2_1/m$		(0,a,0)	(b,0,c)	$a^+b^-c^-$	(0,$\bar{1}$,1)(2,0,0)(0,1,1)	(0,0,0)
15	137 $P4_2/nmc$		(0,a,a)	(b,0,0)	$a^+a^+c^-$	(2,0,0)(0,2,0)(0,0,2)	(0,0,$\bar{1}$)
		Γ_3^+ $q_{tz}q_{oz}$					
16	**123 *P4/mmm***	**(a,0)**†	**(0,0,0)**	**(0,0,0)**	$\boldsymbol{a^0a^0c^0}$‡	**(1,0,0)(0,1,0)(0,0,1)**	**(0,0,0)**
(17)	47 $Pmmm$	(a,b)§	(0,0,0)	(0,0,0)	$a^0b^0c^0$	(1,0,0)(0,1,0)(0,0,1)	(0,0,0)
= 2	127 $P4/mbm$	(a,0)	(b,0,0)	(0,0,0)	$a^0a^0c^+$	(1,1,0)($\bar{1}$,1,0)(0,0,1)	(0,0,0)
= 3	139 $I4/mmm$	($-a/2$,$-a\sqrt{3}/2$)¶	(b,0,b)	(0,0,0)	$a^0b^+b^+$	(0,2,0)(0,0,2)(2,0,0)	($\frac{1}{2}$,$\frac{1}{2}$,$\frac{3}{2}$)
= 5	71 $Immm$	(a,b)	(c,d,e)	(0,0,0)	$a^+b^+c^+$	(2,0,0)(0,2,0)(0,0,2)	($\frac{1}{2}$,$\frac{1}{2}$,$\frac{1}{2}$)
= 6	140 $I4/mcm$	(a,0)	(0,0,0)	(b,0,0)	$a^0a^0c^-$	(1,1,0)($\bar{1}$,1,0)(0,0,2)	(0,0,0)
= 7	74 $Imma$	($-a/2$,$-a\sqrt{3}/2$)	(0,0,0)	(b,0,b)	$a^0b^-b^-$	(0,1,1)(2,0,0)(0,1,$\bar{1}$)	(0,0,0)
= 9	12 $C2/m$	(a,$\bar{b}$)	(0,0,0)	(c,0,d)	$a^0b^-c^-$	(0,$\bar{2}$,0)(2,0,0)(0,1,1)	($\frac{1}{2}$,$\frac{1}{2}$,0)
= 10	15 $C2/c$	($-a/2$,$-a\sqrt{3}/2$)	(0,0,0)	(b,c,b)	$a^-b^-b^-$	(2,$\bar{1}$,$\bar{1}$)(0,1,$\bar{1}$)(0,1,1)	($\frac{1}{2}$,$\frac{1}{2}$,0)
= 11	2 $P\bar{1}$	(a,b)	(0,0,0)	(c,d,e)	$a^-b^-c^-$	(0,1,1)(1,0,1)(1,1,0)	(0,0,0)
= 12	63 $Cmcm$	($-a/2$,$a\sqrt{3}/2$)†† +($b\sqrt{3}/2$,$b/2$)	(0,0,c)	(d,0,0)	$a^0b^+c^-$	(2,0,0)(0,0,$\bar{2}$)(0,2,0)	($\frac{1}{2}$,0,$\frac{1}{2}$)
= 13	62 $Pnma$	($-a/2$,$-a\sqrt{3}/2$)	(0,b,0)	(c,0,c)	$a^+b^-b^-$	(0,1,1)(2,0,0)(0,1,$\bar{1}$)	(0,0,0)
= 14	11 $P2_1/m$	($-a/2$,$-a\sqrt{3}/2$) +($-b\sqrt{3}/2$,$b/2$)	(0,c,0)	(d,0,e)	$a^+b^-c^-$	(0,$\bar{1}$,1)(2,0,0)(0,1,1)	(0,0,0)
= 15	137 $P4_2/nmc$	(a,0)	(b,b,0)	(c,0,0)	$a^+a^+c^-$	(2,0,0)(0,2,0)(0,0,2)	(0,0,$\bar{1}$)
		M_2^+ $q_{1JT}q_{2JT}q_{3JT}$					
18	**127 *P4/mbm***	**(a,0,0)**‡‡	**(0,0,0)**	**(0,0,0)**	$\boldsymbol{a^0a^0c^0}$	**(1,1,0)($\bar{1}$,1,0)(0,0,1)**	**($\frac{1}{2}$,$\frac{1}{2}$,0)**
(19)	139 $I4/mmm$	(a,a,0)	(0,0,0)	(0,0,0)	$a^0b^0a^0$	(0,0,2)(2,0,0)(0,2,0)	(0,0,1)
(20)	204 $Im\bar{3}$	(a,a,a)	(0,0,0)	(0,0,0)	$a^0a^0a^0$	(2,0,0)(0,2,0)(0,0,2)	(0,0,0)
(21)	71 $Immm$	(a,b,c)	(0,0,0)	(0,0,0)	$a^0b^0c^0$	(2,0,0)(0,2,0)(0,0,2)	(0,0,0)
22	55 $Pbam$	(a,0,0)	(b,0,0)	(0,0,0)	$a^0a^0c^+$	(1,1,0)($\bar{1}$,1,0)(0,0,1)	(0,0,0)
23	74 $Imma$	(a,0,0)	(0,b,0)	(0,0,0)	$a^+b^0c^0$	(2,0,0)(0,0,$\bar{2}$)(0,2,0)	(0,0,0)
24	87 $I4/m$	(0,a,0)§§	(b,0,b)	(0,0,0)	$a^0b^+b^+$	(0,0,$\bar{2}$)(0,2,0)(2,0,0)	($\frac{1}{2}$,$-\frac{1}{2}$,$\frac{1}{2}$)
25	12 $C2/m$	(a,0,0)	(b,c,d)	(0,0,0)	$a^+b^+c^+$	(2,$\bar{2}$,0)(0,0,2)(0,$\bar{2}$,0)	($\frac{1}{2}$,$-\frac{1}{2}$,$\frac{1}{2}$)
26	135 $P4_2/mbc$	(a,0,0)	(0,0,0)	(b,0,0)	$a^0a^0c^-$	(1,1,0)($\bar{1}$,1,0)(0,0,2)	($\frac{1}{2}$,$\frac{1}{2}$,0)
27	63 $Cmcm$	(a,0,0)	(0,0,0)	(0,b,0)	$a^-b^0c^0$	(2,0,0)(0,2,0)(0,0,2)	(0,0,0)
= 13	62 $Pnma$	(0,a,0)	(0,b',0)	(c,0,c)¶¶	$a^0b^-b^-$	(0,1,1)(2,0,0)(0,1,$\bar{1}$)	(0,0,0)
28	15 $C2/c$	(a,0,0)	(0,0,0)	(b,0,c)	$a^0b^-c^-$	(0,2,0)($\bar{2}$,0,0)(0,0,2)	(0,0,0)
= 14	11 $P2_1/m$	(0,a,0)	(0,b',0)	(c,0,d)¶¶	$a^0b^-c^-$	(0,$\bar{1}$,1)(2,0,0)(0,1,1)	(0,0,0)
29	14 $P2_1/c$	(0,a,0)	(0,b',0)	(c,d,c)¶¶	$a^-b^-b^-$	(2,0,0)(0,1,$\bar{1}$)(0,1,1)	(0,0,0)
30	2 $P\bar{1}$	(0,a,0)	(0,b',0)	(c,d,e)¶¶	$a^-b^-c^-$	(0,$\bar{1}$,1)(2,0,0)(0,1,1)	(0,0,0)

Calderón *et al.*, 2003; Chapman *et al.*, 2004; Burgy *et al.*, 2004; Ahn *et al.*, 2004, 2005; Goodenough, 2004; Sage *et al.*, 2007; Zhou *et al.*, 2007; Israel *et al.*, 2007; Cox *et al.*, 2008; Horsch *et al.*, 2008). Jahn–Teller distortions of individual octahedra, ordering and tilting of the octahedra, magnetic ordering and phase separation are invariably accompanied by lattice distortions at a range of length scales. Changes associated with discrete phase transitions appear overtly as changes in lattice parameters, and these can be described formally in terms of macroscopic strains. The second objective of the present study, therefore, was to analyse strain/order-parameter coupling for combined Jahn–Teller and octahedral tilting transitions, following the approach set out by Carpenter *et al.* (1999, 2001, 2005) and Carpenter (2007).

This paper is the first of two on the symmetry and coupling behaviour of perovskites with both octahedral tilting and Jahn–Teller transitions. Here, a group-theoretical treatment of coupling between 15 possible tilt systems and three Jahn–Teller ordering schemes is presented in §2. Readers who are not interested in the derivations might choose to go directly to the tables which summarize the space groups, order parameters and lattice geometry of the possible structure types which are predicted. §3 contains a formal treatment of coupling between different order parameters and macroscopic strains in the mixed structures, and the resulting relationships are presented as a series of equations, based on Landau theory. These general equations provide the basis for analysing changes in lattice parameters of real materials, particularly from high-resolution diffraction experiments, to determine the evolution of individual tilting or Jahn–Teller order parameters and to investigate the manner in which the separate processes influence each other. §4 deals with the permitted thermodynamic character of phase transitions in mixed systems when tilting precedes or follows a Jahn–Teller transition. The behaviour of a few well known phases is reviewed in the context of the group-theoretical results. §5 is a brief introduction to the additional role

Table 1 (continued)

	Space group		M_3^+ $q_1q_2q_3$	R_4^+ $q_4q_5q_6$	System	Lattice vectors	Origin
31	52 *Pnna*	(*a*,0,0)	(0,0,*b*)	(*c*,0,0)	$a^0b^+c^-$	(0,0,2)(0,2,0)($\bar{2}$,0,0)	(0,0,0)
32	62 *Pnma*	(0,*a*,0)	(0,0,*b*)	(*c*,0,0)	$a^0b^+c^-$	(0,2,0)($\bar{2}$,0,0)(0,0,2)	(0,0,0)
= 13	62 *Pnma*	(0,*a*,0)	(0,*b*,0)	(*c*,0,*c*)	$a^+b^-b^-$	(0,1,1)(2,0,0)(0,1,$\bar{1}$)	(0,0,0)
= 14	11 $P2_1/m$	(0,*a*,0)	(0,*b*,0)	(*c*,0,*d*)	$a^+b^-c^-$	(0,$\bar{1}$,1)(2,0,0)(0,1,1)	(0,0,0)
33	86 $P4_2/n$	(*a*,0,0)	(0,*b*,*b*)	(*c*,0,0)	$a^+a^+c^-$	(0,2,0)($\bar{2}$,0,0)(0,0,2)	(0,0,0)
		R_3^+ $q_{4JT}q_{5JT}$					
34	**140 *I4/mcm***	**(0,*a*)†††**	**(0,0,0)**	**(0,0,0)**	$\boldsymbol{a^0a^0c^0}$	**(1,1,0)($\bar{1}$,1,0)(0,0,2)**	**($\frac{1}{2}$, $\frac{1}{2}$,0)**
(35)	139 *I4/mmm*	(*a*,0)	(0,0,0)	(0,0,0)	$a^0a^0c^0$	(1,1,0)($\bar{1}$,1,0)(0,0,2)	(0,0,0)
(36)	69 *Fmmm*	(*a*,*b*)	(0,0,0)	(0,0,0)	$a^0b^0c^0$	(2,0,0)(0,2,0)(0,0,2)	(0,0,0)
37	135 $P4_2/mbc$	(0,*a*)	(*b*,0,0)	(0,0,0)	$a^0a^0c^+$	(1,1,0)($\bar{1}$,1,0)(0,0,2)	(0,0,0)
38	126 *P4/nnc*	($a\sqrt{3}/2$,−*a*/2)‡‡‡	(*b*,0,*b*)	(0,0,0)	$a^0b^+b^+$	(0,2,0)(0,0,2)(2,0,0)	(0,1,0)
39	48 *Pnnn*	(*a*,*b*)	(*c*,*d*,*e*)	(0,0,0)	$a^+b^+c^+$	(2,0,0)(0,2,0)(0,0,2)	(0,0,0)
40	72 *Ibam*	(0,*a*)	(0,0,0)	(*b*,0,0)	$a^0a^0c^-$	(1,1,0)($\bar{1}$,1,0)(0,0,2)	(0,0,0)
= 10	15 $C2/c$	($a\sqrt{3}/2$,−*a*/2)	(0,0,0)	(*b*,*c*,*b*)	$a^-b^-b^-$	(2,$\bar{1}$,$\bar{1}$)(0,1,$\bar{1}$)(0,1,1)	($\frac{1}{2}$,$\frac{1}{2}$,0)
= 11	2 $P\bar{1}$	(*b*,*a*)	(0,0,0)	(*c*,*d*,*e*)	$a^-b^-c^-$	(0,1,1)(1,0,1)(1,1,0)	(0,0,0)
41	15 $C2/c$	(−*a*/2,*a*$\sqrt{3}$/2) +(*b*$\sqrt{3}$/2,*b*/2)§§§	(0,0,*c*)	(*d*,0,0)	$a^0b^+c^-$	($\bar{2}$,0,0)(0,0,2)(0,2,0)	($\frac{1}{2}$,0,$\frac{1}{2}$)
42	14 $P2_1/c$	($a\sqrt{3}/2$,−*a*/2)	(0,*b*,0)	(*c*,*d*,*c*)	$a^\pm b^-b^-$	(2,0,0)(0,1,$\bar{1}$)(0,1,1)	(0,0,0)
	14 $P\,1\,1\,2_1/a$	($a\sqrt{3}/2$,−*a*/2)	(0,*b*,0)	(*c*,*d*,*c*)	$a^\pm b^-b^-$	(0,1,1)(2,0,0)(0,1,$\bar{1}$)	(0,0,0)
43	2 $P\bar{1}$	(−*a*/2,−*a*$\sqrt{3}$/2) +(*b*$\sqrt{3}$/2,−*b*/2)	(0,*c*,0)	(*d*,*e*,*f*)	$a^\pm b^-c^-$	(0,$\bar{1}$,1)(2,0,0)(0,1,1)	(0,0,0)
44	68 *Ccca*	(0,*a*)	(0,*b*,*b*)	(*c*,0,0,)	$a^+a^+c^-$	(2,2,0)($\bar{2}$,2,0)(0,0,2)	(0,0,0)

† The JT distortion here acts to make the *z* direction unique. ‡ Here and subsequently we use different literals for different axes distinguished by the Jahn–Teller distortion, even when these are not distinguished by tilting. § This JT distortion would make the three axes unequal. ¶ This is JT acting along the *x* direction of the starting cell. †† This is JT acting along the *y* direction of the starting cell. ‡‡ The JT acts to distort octahedra in the plane perpendicular to *z* of the starting cell. §§ The JT acts to distort octahedra in the plane perpendicular to *x* of the starting cell. ¶¶ The addition of prime to *b* signifies that this component is a secondary order parameter. The Glazer tilt scheme is given for $b' = 0$. ††† The JT acts to distort octahedra in the plane perpendicular to *z* of the starting cell. ‡‡‡ The JT acts to distort octahedra in the plane perpendicular to *x* of the starting cell. §§§ This term acts to distort octahedra in the plane perpendicular to *y* of the starting cell.

that cation ordering might play. Practical applications of the formal results from this paper (paper I) are illustrated for selected vanadate, manganite, aluminate and cobaltate perovskites in the second paper of the series (paper II, Carpenter & Howard, 2009).

2. Symmetry rules: permitted Jahn–Teller + tilt systems

Use of the group theory program *ISOTROPY* (Stokes *et al.*, 2007) provides a straightforward means of enumerating the permitted space groups and their non-zero order parameters for materials which combine Jahn–Teller and tilting distortions. Here the approach of Howard & Stokes (1998, 2004, 2005), Stokes *et al.* (2002), Howard *et al.* (2003) and Howard & Zhang (2004*a*,*b*) is followed in using *ISOTROPY* to consider all possible couplings of three Jahn–Teller ordering schemes with 15 *R*-point and *M*-point tilt systems in ABX_3 perovskites.[1] Phase transitions between the different structures can be understood in terms of symmetry hierarchies, with second-order character allowed for particular changes of space group.

Table 1 lists the order-parameter relationships and space groups given by *ISOTROPY* for possible structures which could arise by combining Jahn–Teller (orbital) ordering instabilities with octahedral tilting instabilities. The reference structure, for which all order parameters are strictly zero, is the ideal cubic perovskite in the space group $Pm\bar{3}m$, set with the octahedrally coordinated *B* cation at the origin. The three 'pure' Jahn–Teller structures, *i.e.* without any tilting, are associated with active irreducible representations (irreps) Γ_3^+, M_2^+ and R_3^+. These are two-, three- and two-dimensional irreps, respectively, and the pure JT structures are obtained for particular choices of the corresponding order parameters. Γ_3^+ with order parameter (*a*,0) corresponds to the structure with the unique direction of Q_3-distorted BX_6 octahedra all pointing in the same direction. M_2^+ (*a*,0,0) corresponds to the *d*-type structure, while R_3^+ (0,*a*) corresponds to the *a*-type structure. The 15 tilt systems considered here are associated with active representations M_3^+, R_4^+ and M_3^+ + R_4^+, as set out in Howard & Stokes (1998). Glazer notation for these tilt systems is also given in Table 1 under the heading 'System'. The unit cell can be identified in each case by reference to the column 'Lattice vectors'. For example, (1,1,0)($\bar{1}$, 1,0)(0,0,2) implies a cell with dimensions close to $\sqrt{2}a_p \times \sqrt{2}a_p \times 2a_p$, where a_p represents the lattice parameter of the primitive cubic reference structure.

Rather than including the complete *ISOTROPY* list for every single combination of Γ_3^+, M_2^+, R_3^+ with M_3^+ and R_4^+, a subset has been selected to represent the structure types most likely to develop in real materials. These have order-parameter components consistent with the pure JT distortions referred to above. In coupling Γ_3^+ with M_3^+, for example, structures with order parameter (*a*,0) for Γ_3^+ are retained. Structure types with a non-zero second component have been omitted except where symmetry reduction due to tilting permits a second component of the order parameter to be non-zero. The latter have JT order-parameter components (*a*,*b*), but the value of *b* is presumed to be small. In addition, it was the practice of Howard & Stokes (1998, 2004, 2005) to remove structures showing 'in-phase' (M_3^+) and 'out-of-phase' (R_4^+) tilts around the same axis, *i.e.* structures with corresponding components of order parameters being both non-zero. These have again been removed here, except when coupling M_3^+ and R_4^+ with R_3^+ where it was found that symmetry lowering due to the JT distortion permits a

[1] The reader unfamiliar with this approach may wish to consult the review article by Howard & Stokes (2005). There is, however, an error in this article in that Table 3 shows the irrep associated with the distortion in the *I*4/*mcm* structure of $KCuF_3$ to be R_4^+ when it should be R_3^+.

Table 2
A summary of space-group changes which can occur when three different JT ordering schemes are superimposed on 15 separate tilt systems.

'No change' signifies that Jahn–Teller ordering can occur in a given tilted structure without any symmetry reduction. 'None' signifies that there are no structures with both JT order and the given tilt system. Isosymmetric transitions must be first order in character and the $Pm\bar{3}m \leftrightarrow P4/mmm$ transition is first order due to the existence of third-order invariants in the order parameter. The remaining transitions can be second order.

Tilt system (Glazer notation)	No JT	Γ_3^+	M_2^+	R_3^+
$a^0a^0a^0$	$Pm\bar{3}m$	$P4/mmm$	$P4/mbm$	$I4/mcm$
$a^0a^0c^+$	$P4/mbm$	No change	$Pbam$ $Imma$	$P4_2/mbc$
$a^0b^+b^+$	$I4/mmm$	No change	$I4/m$	$P4/nnc$
$a^+a^+a^+$	$Im\bar{3}$	None	None	None
$a^+b^+c^+$	$Immm$	No change	$C2/m$	$Pnnn$
$a^0a^0c^-$	$I4/mcm$	No change	$P4_2/mnc$ $Cmcm$	$Ibam$
$a^0b^-b^-$	$Imma$	No change	$Pnma$	None
$a^-a^-a^-$	$R\bar{3}c$	None	None	None
$a^0b^-c^-$	$C2/m$	No change	$C2/c$ $P2_1/m$	None
$a^-b^-b^-$	$C2/c$	No change	$P2_1/c$	No change
$a^-b^-c^-$	$P\bar{1}$	No change	$P\bar{1}$	No change
$a^0b^+c^-$	$Cmcm$	No change	$Pnna$ $Pnma$	$C2/c$
$a^+b^-b^-$	$Pnma$	No change	No change	$P2_1/c$†
$a^+b^-c^-$	$P2_1/m$	No change	No change	$P\bar{1}$†
$a^+a^+c^-$	$P4_2/nmc$	No change	$P4_2/n$	$Ccca$

† In these structures there is, along with the in-phase (+) tilt around the X axis, a component of out-of-phase (−) tilt which can be and presumably is non-zero.

component of out-of-phase tilting (not necessarily large) around an axis of formerly pure 'in-phase' tilts.

Each structure-type listed in Table 1 has been assigned a reference or sequence number. Structures #1–15 are the tilted structures obtained in the absence of JT distortion, as have been tabulated previously (Howard & Stokes, 1998). The three pure JT structures are highlighted in bold. In a number of instances, the JT distortion can be accommodated in a tilted structure without changing either the unit cell or the space-group symmetry. These are identified in the reference column by the sequence number of the pertinent tilted structure. Finally, as detailed in the footnotes, some alternative combinations of order parameters are shown for different directions of the unique JT axis. As an example of this, the order parameter for irrep Γ_3^+ appears as both $(a,0)$ and $\left(-\frac{a}{2}, -\frac{a\sqrt{3}}{2}\right)$ according to whether the unique axis of the Jahn–Teller distortion is along Z or X of the reference system used in *ISOTROPY*. The need to invoke different unique axes for the JT distortion arises because the orientation of tilts from the pure tilting systems (#1–15) have been preserved in the mixed Jahn–Teller + tilt structures.

For four of the space groups in the M_2^+ set, the lowering of symmetry driven by combining M_2^+ and R_4^+ distortions permits the M_3^+ components to be non-zero without further symmetry reduction. The M_3^+ components can be understood as being secondary order parameters in that they are simply a consequence of the symmetry already being lowered, and are indicated by b' rather than b in Table 1. Similarly, $P2_1/c$ obtained by M_2^+ and R_4^+ as the driving order parameters can have non-zero values of secondary order parameter components belonging to R_3^+, while $P2_1/c$ driven by R_3^+, M_3^+ and R_4^+ can have secondary M_2^+ components. Formally, the structures in the space group $P2_1/c$ listed as numbers 29 and 42 in Table 1 are the same, but the former is expected to have the secondary R_3^+ component $\simeq 0$ and the latter is expected to have the secondary M_2^+ component $\simeq 0$. The same argument applies to structures in the space group $P\bar{1}$ listed as numbers 30 and 43. It should also be noted that if the secondary order parameter is zero at high temperatures but adopts non-zero values below some critical temperature it becomes, in effect, the driving order parameter for an isosymmetric phase transition.

Table 2 contains a subset of the results listed in Table 1. It provides a summary of possible space groups for structures in which each of the tetragonal $P4/mmm$ (Γ_3^+), $P4/mbm$ (M_2^+) and $I4/mcm$ (R_3^+) JT ordering schemes is imposed on each of the 15 tilted structures. 'No change' signifies that there need be no change in space group (or unit cell) when the Jahn–Teller distortions are added. In other words, the orbital ordering scheme is compatible with the tilt system and can develop without changing the geometry of the tilting. This does not preclude the possibility that the Jahn–Teller distortion might drive the structure to another tilting system of lower symmetry. 'None' signifies that there are no structures which can combine orbital ordering with the specified tilting. This applies to all the trigonal structures and is a consequence of the incompatibility of a threefold axis with tetragonal or orthorhombic distortions of individual octahedra. Again, however, there remains the possibility that a Jahn–Teller distortion could develop which would drive the structure to adopt a tilt system of lower symmetry. In the remaining combinations, development of JT distortions in a perovskite with tilted octahedra would cause a reduction in symmetry. In a few cases, more than one structure is possible in a given tilt system, depending on the orientation of the unique Jahn–Teller direction relative to the axes of tilt.

3. Permitted strain/order-parameter relationships

Although the driving mechanism for Jahn–Teller transitions is an instability of the electronic structure of individual cations, phase transitions become manifest macroscopically through the preferred alignments of distorted coordination octahedra. The geometrical meaning of the order-parameter components, q_i, can conveniently be considered in relation to the usual two limiting cases. In the displacive limit, individual octahedra would all deform through a range of dimensions in proportion to the splitting of d-orbitals. The magnitude of q_i would be related to the amount of distortion from perfect octahedral geometry. In the order/disorder limit, octahedra are distorted by a fixed amount but are randomly oriented in the high-

temperature form and become ordered in the low-temperature form. The magnitude of q_i would be given by the proportion of octahedra in their ordered configuration. Real behaviour might be intermediate between these but there will always be a clear relationship between the magnitude of q_i and changes in lattice parameters, as expressed in terms of spontaneous strains, e_k. Symmetry rules determine the nature of coupling between q_i and e_k, so that the strains can be used to follow the evolution of individual order-parameter components explicitly. An orthorhombic strain is commonly used to describe lattice distortions of Jahn–Teller systems (*e.g.* Alonso *et al.*, 2000; Horsch *et al.*, 2008; Martínez-Lope *et al.*, 2008), but this has not previously been expressed in terms of any specific combination of order-parameter components.

From Carpenter *et al.* (2001) and Carpenter (2007), the spontaneous strains accompanying M_3^+ and R_4^+ tilting transitions are

$$\begin{aligned} e_\mathrm{a} &= e_1 + e_2 + e_3 \\ &= -\left[\frac{\lambda_1\left(q_1^2+q_2^2+q_3^2\right)+\lambda_2\left(q_4^2+q_5^2+q_6^2\right)}{\frac{1}{3}\left(C_{11}^\mathrm{o}+2C_{12}^\mathrm{o}\right)}\right] \end{aligned} \quad (1)$$

$$e_\mathrm{oz} = e_1 - e_2 = -\left[\frac{\lambda_3\sqrt{3}\left(q_2^2-q_3^2\right)+\lambda_4\sqrt{3}\left(q_5^2-q_6^2\right)}{\frac{1}{2}\left(C_{11}^\mathrm{o}-C_{12}^\mathrm{o}\right)}\right] \quad (2)$$

$$\begin{aligned} e_\mathrm{tz} &= \frac{1}{\sqrt{3}}\left(2e_3 - e_1 - e_2\right) \\ &= -\left[\frac{\lambda_3\left(2q_1^2-q_2^2-q_3^2\right)+\lambda_4\left(2q_4^2-q_5^2-q_6^2\right)}{\frac{1}{2}\left(C_{11}^\mathrm{o}-C_{12}^\mathrm{o}\right)}\right] \end{aligned} \quad (3)$$

$$e_4 = -\frac{\lambda_5 q_4 q_6}{2\lambda_6\left(q_1^2+q_2^2+q_3^2\right)+2\lambda_7 q_2^2+C_{44}^\mathrm{o}} \quad (4)$$

$$e_5 = -\frac{\lambda_5 q_4 q_5}{2\lambda_6\left(q_1^2+q_2^2+q_3^2\right)+2\lambda_7 q_3^2+C_{44}^\mathrm{o}} \quad (5)$$

$$e_6 = -\frac{\lambda_5 q_5 q_6}{2\lambda_6\left(q_1^2+q_2^2+q_3^2\right)+2\lambda_7 q_1^2+C_{44}^\mathrm{o}}. \quad (6)$$

Equations (4)–(6) can be simplified by assuming $C_{44}^\mathrm{o} >> \left(2\lambda_6\left(q_1^2+q_2^2+q_3^2\right)+2\lambda_7 q_i^2\right)$, $i = 1$, 2 or 3, so that

$$e_4 = -\frac{\lambda_5 q_4 q_6}{C_{44}^\mathrm{o}} \quad (7)$$

$$e_5 = -\frac{\lambda_5 q_4 q_5}{C_{44}^\mathrm{o}} \quad (8)$$

$$e_6 = -\frac{\lambda_5 q_5 q_6}{C_{44}^\mathrm{o}}. \quad (9)$$

The order-parameter components q_1–q_3 are for M_3^+ and q_4–q_6 are for R_4^+. Linear strains e_1, e_2 and e_3 are parallel to reference axes X, Y, Z, and the subscript z specifies the unique tetragonal axis as being parallel to Z of the reference system. These combinations lead to distinctive patterns of lattice distortions according to which of the six order-parameter components are non-zero.

The complete Landau expansion given by Carpenter *et al.* (2001) for $M_3^+ + R_4^+$ tilting transitions could easily be extended to include all components of the JT transitions, but the resulting expansion for the most general cases would be rather long. As a simplification, coupling of strains with JT order parameters is considered separately for Γ_3^+, M_2^+ and R_3^+ as the active representations. In JT + tilt systems there are then a few further coupling terms to be considered.

Landau expansions for the active representations, Γ_3^+, M_2^+ and R_3^+, are, respectively

$$\begin{aligned} G_{\Gamma 3+} = {} & \frac{1}{2}a\Theta_\mathrm{s}\left(\coth\left(\frac{\Theta_\mathrm{s}}{T}\right)-\coth\left(\frac{\Theta_\mathrm{s}}{T_{\mathrm{c,JT}}}\right)\right)\left(q_\mathrm{tz}^2+q_\mathrm{oz}^2\right) \\ & +\frac{1}{3}uq_\mathrm{tz}\left(q_\mathrm{tz}^2-3q_\mathrm{oz}^2\right)+\frac{1}{4}b\left(q_\mathrm{tz}^2+q_\mathrm{oz}^2\right)^2 \\ & +\frac{1}{3}vq_\mathrm{tz}\left(q_\mathrm{tz}^2-3q_\mathrm{oz}^2\right)\left(q_\mathrm{tz}^2+q_\mathrm{oz}^2\right) \\ & +\frac{1}{6}c\left(q_\mathrm{tz}^2+q_\mathrm{oz}^2\right)^3+\frac{1}{6}c'q_\mathrm{tz}^2\left(q_\mathrm{tz}^2-3q_\mathrm{oz}^2\right)^2 \\ & +\lambda_{\mathrm{t}\Gamma 3+}\left(q_\mathrm{oz}e_\mathrm{oz}-q_\mathrm{tz}e_\mathrm{tz}\right)+\lambda_{\mathrm{a}\Gamma 3+}e_\mathrm{a}\left(q_\mathrm{tz}^2+q_\mathrm{oz}^2\right) \\ & +\lambda_{\mathrm{e}\Gamma 3+}\left(q_\mathrm{tz}\left(2e_6^2-e_4^2-e_5^2\right)-\sqrt{3}q_\mathrm{oz}\left(e_4^2-e_5^2\right)\right) \\ & +\frac{1}{4}\left(C_{11}^\mathrm{o}-C_{12}^\mathrm{o}\right)\left(e_\mathrm{oz}^2+e_\mathrm{tz}^2\right)+\frac{1}{6}\left(C_{11}^\mathrm{o}+2C_{12}^\mathrm{o}\right)e_\mathrm{a}^2 \\ & +\frac{1}{2}C_{44}^\mathrm{o}\left(e_4^2+e_5^2+e_6^2\right) \end{aligned} \quad (10)$$

$$\begin{aligned} G_{\mathrm{M}2+} = {} & \frac{1}{2}a\Theta_\mathrm{s}\left(\coth\left(\frac{\Theta_\mathrm{s}}{T}\right)-\coth\left(\frac{\Theta_\mathrm{s}}{T_{\mathrm{c,JT}}}\right)\right)\left(q_{1\mathrm{JT}}^2+q_{2\mathrm{JT}}^2+q_{3\mathrm{JT}}^2\right) \\ & +\frac{1}{4}b\left(q_{1\mathrm{JT}}^2+q_{2\mathrm{JT}}^2+q_{3\mathrm{JT}}^2\right)^2 \\ & +\frac{1}{4}b'\left(q_{1\mathrm{JT}}^4+q_{2\mathrm{JT}}^4+q_{3\mathrm{JT}}^4\right)+\frac{1}{6}c\left(q_{1\mathrm{JT}}^2+q_{2\mathrm{JT}}^2+q_{3\mathrm{JT}}^2\right)^3 \\ & +\frac{1}{6}c'\left(q_{1\mathrm{JT}}q_{2\mathrm{JT}}q_{3\mathrm{JT}}\right)^2 \\ & +\frac{1}{6}c''\left(q_{1\mathrm{JT}}^2+q_{2\mathrm{JT}}^2+q_{3\mathrm{JT}}^2\right)\left(q_{1\mathrm{JT}}^4+q_{2\mathrm{JT}}^4+q_{3\mathrm{JT}}^4\right) \\ & +\lambda_{\mathrm{aM}2+}e_\mathrm{a}\left(q_{1\mathrm{JT}}^2+q_{2\mathrm{JT}}^2+q_{3\mathrm{JT}}^2\right) \\ & +\lambda_{\mathrm{tM}2+}\left[\sqrt{3}e_\mathrm{oz}\left(q_{2\mathrm{JT}}^2-q_{3\mathrm{JT}}^2\right)+e_\mathrm{tz}\left(2q_{1\mathrm{JT}}^2-q_{2\mathrm{JT}}^2-q_{3\mathrm{JT}}^2\right)\right] \\ & +\lambda_{\mathrm{e}1\mathrm{M}2+}\left(q_{1\mathrm{JT}}^2+q_{2\mathrm{JT}}^2+q_{3\mathrm{JT}}^2\right)\left(e_4^2+e_5^2+e_6^2\right) \\ & +\lambda_{\mathrm{e}2\mathrm{M}2+}\left(q_{1\mathrm{JT}}^2e_6^2+q_{2\mathrm{JT}}^2e_4^2+q_{3\mathrm{JT}}^2e_5^2\right) \\ & +\frac{1}{4}\left(C_{11}^\mathrm{o}-C_{12}^\mathrm{o}\right)\left(e_\mathrm{oz}^2+e_\mathrm{tz}^2\right)+\frac{1}{6}\left(C_{11}^\mathrm{o}+2C_{12}^\mathrm{o}\right)e_\mathrm{a}^2 \\ & +\frac{1}{2}C_{44}^\mathrm{o}\left(e_4^2+e_5^2+e_6^2\right) \end{aligned} \quad (11)$$

$$G_{\mathrm{R3+}} = \frac{1}{2}a\Theta_{\mathrm{s}}\left(\coth\left(\frac{\Theta_{\mathrm{s}}}{T}\right) - \coth\left(\frac{\Theta_{\mathrm{s}}}{T_{\mathrm{c,JT}}}\right)\right)\left(q_{\mathrm{4JT}}^2 + q_{\mathrm{5JT}}^2\right) + \frac{1}{4}b\left(q_{\mathrm{4JT}}^2 + q_{\mathrm{5JT}}^2\right)^2 + \frac{1}{6}c\left(q_{\mathrm{4JT}}^2 + q_{\mathrm{5JT}}^2\right)^3 + \frac{1}{6}c'\left(11q_{\mathrm{4JT}}^6 + 15q_{\mathrm{4JT}}^4q_{\mathrm{5JT}}^2 + 45q_{\mathrm{4JT}}^2q_{\mathrm{5JT}}^4 + 9q_{\mathrm{5JT}}^6\right) + \lambda_{\mathrm{aR3+}}e_{\mathrm{a}}\left(q_{\mathrm{4JT}}^2 + q_{\mathrm{5JT}}^2\right) + \lambda_{\mathrm{tR3+}}\left[2e_{\mathrm{oz}}q_{\mathrm{4JT}}q_{\mathrm{5JT}} + e_{\mathrm{tz}}\left(q_{\mathrm{4JT}}^2 - q_{\mathrm{5JT}}^2\right)\right] + \lambda_{\mathrm{e1R3+}}\left(q_{\mathrm{4JT}}^2 + q_{\mathrm{5JT}}^2\right)\left(e_4^2 + e_5^2 + e_6^2\right) + \lambda_{\mathrm{e2R3+}}\left[q_{\mathrm{4JT}}^2\left(4e_6^2 + e_4^2 + e_5^2\right) + 3q_{\mathrm{5JT}}^2\left(e_4^2 + e_5^2\right) + 2\sqrt{3}q_{\mathrm{4JT}}q_{\mathrm{5JT}}\left(e_4^2 - e_5^2\right)\right] + \frac{1}{4}(C_{11}^{\mathrm{o}} - C_{12}^{\mathrm{o}})\left(e_{\mathrm{oz}}^2 + e_{\mathrm{tz}}^2\right) + \frac{1}{6}(C_{11}^{\mathrm{o}} + 2C_{12}^{\mathrm{o}})e_{\mathrm{a}}^2 + \frac{1}{2}C_{44}^{\mathrm{o}}\left(e_4^2 + e_5^2 + e_6^2\right). \quad (12)$$

The order parameter components for Γ_3^+ are specified as q_{tz} and q_{oz}, following Carpenter *et al.* (2005); q_{1JT}, q_{2JT} and q_{3JT} have been assigned to M_2^+ and q_{4JT}, q_{5JT} to R_3^+. Terms in q are included to sixth order, terms in e to second order, and coupling terms to the lowest order permitted by symmetry. The reference system from *ISOTROPY* is used throughout for definition of the strains.

In systems without octahedral tilting, the (symmetry-breaking) tetragonal shear strains scale with non-zero order-parameter components as

$$e_{\mathrm{tz}\Gamma\mathrm{3+}} = \frac{\lambda_{\mathrm{t}\Gamma\mathrm{3+}}q_{\mathrm{tz}}}{\frac{1}{2}\left(C_{11}^{\mathrm{o}} - C_{12}^{\mathrm{o}}\right)} \quad (13)$$

$$e_{\mathrm{tzM2+}} = \frac{-\lambda_{\mathrm{tM2+}}\left(2q_{\mathrm{1JT}}^2 - q_{\mathrm{2JT}}^2 - q_{\mathrm{3JT}}^2\right)}{\frac{1}{2}\left(C_{11}^{\mathrm{o}} - C_{12}^{\mathrm{o}}\right)} \quad (14)$$

$$e_{\mathrm{tzR3+}} = \frac{-\lambda_{\mathrm{tR3+}}\left(q_{\mathrm{4JT}}^2 - q_{\mathrm{5JT}}^2\right)}{\frac{1}{2}\left(C_{11}^{\mathrm{o}} - C_{12}^{\mathrm{o}}\right)}. \quad (15)$$

The corresponding orthorhombic strains are

$$e_{\mathrm{oz}\Gamma\mathrm{3+}} = \frac{-\lambda_{\mathrm{t}\Gamma\mathrm{3+}}q_{\mathrm{oz}}}{\frac{1}{2}\left(C_{11}^{\mathrm{o}} - C_{12}^{\mathrm{o}}\right)} \quad (16)$$

$$e_{\mathrm{ozM2+}} = \frac{-\sqrt{3}\lambda_{\mathrm{tM2+}}\left(q_{\mathrm{2JT}}^2 - q_{\mathrm{3JT}}^2\right)}{\frac{1}{2}\left(C_{11}^{\mathrm{o}} - C_{12}^{\mathrm{o}}\right)} \quad (17)$$

$$e_{\mathrm{ozR3+}} = \frac{-2\lambda_{\mathrm{tR3+}}q_{\mathrm{4JT}}q_{\mathrm{5JT}}}{\frac{1}{2}\left(C_{11}^{\mathrm{o}} - C_{12}^{\mathrm{o}}\right)}. \quad (18)$$

Volume strains, e_{a}, due to coupling with each set of order-parameter components are

$$e_{\mathrm{a}\Gamma\mathrm{3+}} = \frac{-\lambda_{\mathrm{a}\Gamma\mathrm{3+}}\left(q_{\mathrm{tz}}^2 + q_{\mathrm{oz}}^2\right)}{\frac{1}{3}\left(C_{11}^{\mathrm{o}} + 2C_{12}^{\mathrm{o}}\right)} \quad (19)$$

$$e_{\mathrm{aM2+}} = \frac{-\lambda_{\mathrm{aM2+}}\left(q_{\mathrm{1JT}}^2 + q_{\mathrm{2JT}}^2 + q_{\mathrm{3JT}}^2\right)}{\frac{1}{3}\left(C_{11}^{\mathrm{o}} + 2C_{12}^{\mathrm{o}}\right)} \quad (20)$$

$$e_{\mathrm{aR3+}} = \frac{-\lambda_{\mathrm{aR3+}}\left(q_{\mathrm{4JT}}^2 + q_{\mathrm{5JT}}^2\right)}{\frac{1}{3}\left(C_{11}^{\mathrm{o}} + 2C_{12}^{\mathrm{o}}\right)}. \quad (21)$$

It is also necessary to consider contributions to the excess free energy of strain coupling terms which include a strain component and a single order parameter from each of the tilt and JT systems. According to *ISOTROPY*, there are no terms of the form $e_{\mathrm{tz}}q_{\mathrm{JT}}q_{\mathrm{tilt}}$ or $e_{\mathrm{oz}}q_{\mathrm{JT}}q_{\mathrm{tilt}}$. Similarly, there are no terms of the form $e_iq_{\mathrm{JT}}q_{\mathrm{tilt}}$, where i = 4, 5 or 6, if q_{JT} is from M_2^+ and q_{tilt} is from R_4^+ or if q_{JT} is from R_3^+ and q_{tilt} is from M_3^+. There are terms which transform as $\Gamma_5^+\oplus M_2^+\oplus M_3^+$ and $\Gamma_5^+\oplus R_3^+\oplus R_4^+$, however, and these are, respectively, $\lambda_{\mathrm{eM2+M3+}}(e_6q_{\mathrm{1JT}}q_1 + e_4q_{\mathrm{2JT}}q_2 + e_5q_{\mathrm{3JT}}q_3)$ and $\lambda_{\mathrm{eR3+R4+}}(e_6q_{\mathrm{5JT}}q_4 + \frac{\sqrt{3}}{2}e_4q_{\mathrm{4JT}}q_5 - \frac{1}{2}e_4q_{\mathrm{5JT}}q_5 - \frac{\sqrt{3}}{2}e_5q_{\mathrm{4JT}}q_6 - \frac{1}{2}e_5q_{\mathrm{5JT}}q_6)$. For the case of Γ_3^+ as the active Jahn–Teller representation, a check with *ISOTROPY* revealed that there are no equivalent coupling terms in e_i (i = 4, 5, 6), q_{JT} and q_{tilt} if q_{tilt} is from either M_3^+ or R_4^+ (*i.e.* $\Gamma_5^+\oplus\Gamma_3^+\oplus M_3^+$ or $\Gamma_5^+\oplus\Gamma_3^+\oplus R_4^+$).

Making the same assumption as before in relation to deriving (7)–(9) from (4)–(6), *i.e.* that coupling terms of the form λe^2q^2 are negligibly small in comparison with $\frac{1}{2}C^{\mathrm{o}}e^2$, leads to the strain relations for M_2^+ (JT) + M_3^+ (tilting), together with R_4^+ (tilting)

$$e_4 = \frac{-\lambda_5q_4q_6 - \lambda_{\mathrm{eM2+M3+}}q_{\mathrm{2JT}}q_2}{C_{44}^{\mathrm{o}}} \quad (22)$$

$$e_5 = \frac{-\lambda_5q_4q_5 - \lambda_{\mathrm{eM2+M3+}}q_{\mathrm{3JT}}q_3}{C_{44}^{\mathrm{o}}} \quad (23)$$

$$e_6 = \frac{-\lambda_5q_5q_6 - \lambda_{\mathrm{eM2+M3+}}q_{\mathrm{1JT}}q_1}{C_{44}^{\mathrm{o}}} \quad (24)$$

and, for R_3^+ (JT) + R_4^+ (tilting)

$$e_4 = \frac{-\lambda_5q_4q_6 - \frac{\sqrt{3}}{2}\lambda_{\mathrm{eR3+R4+}}q_{\mathrm{4JT}}q_5 + \frac{1}{2}\lambda_{\mathrm{eR3+R4+}}q_{\mathrm{5JT}}q_5}{C_{44}^{\mathrm{o}}} \quad (25)$$

$$e_5 = \frac{-\lambda_5q_4q_5 + \frac{\sqrt{3}}{2}\lambda_{\mathrm{eR3+R4+}}q_{\mathrm{4JT}}q_6 + \frac{1}{2}\lambda_{\mathrm{eR3+R4+}}q_{\mathrm{5JT}}q_6}{C_{44}^{\mathrm{o}}} \quad (26)$$

$$e_6 = \frac{-\lambda_5q_5q_6 - \lambda_{\mathrm{eR3+R4+}}q_{\mathrm{5JT}}q_4}{C_{44}^{\mathrm{o}}}. \quad (27)$$

Finally, and for completeness, it is necessary to add coupling terms which determine the way in which the Jahn–Teller and tilting processes might interact directly, rather than indirectly through common strains. For systems with Γ_3^+ JT + tilting, these will contribute to the excess free energy as

$$\lambda_{\mathrm{q}\Gamma\mathrm{3+M3+}}\left[q_{\mathrm{tz}}\left(2q_1^2 - q_2^2 - q_3^2\right) + \sqrt{3}q_{\mathrm{oz}}\left(q_3^2 - q_2^2\right)\right] + \lambda_{\mathrm{q}\Gamma\mathrm{3+R4+}}\left[q_{\mathrm{tz}}\left(2q_4^2 - q_5^2 - q_6^2\right) + \sqrt{3}q_{\mathrm{oz}}\left(q_6^2 - q_5^2\right)\right]. \quad (28)$$

For M_2^+ JT + tilting, the direct coupling terms in the excess free energy are

$$\lambda_{qM2+M3+}\left(q_{1JT}^2+q_{2JT}^2+q_{3JT}^2\right)\left(q_1^2+q_2^2+q_3^2\right)$$
$$+\lambda'_{qM2+M3+}\left(q_{1JT}^2q_1^2+q_{2JT}^2q_2^2+q_{3JT}^2q_3^2\right)$$
$$+\lambda_{qM2+R4+}\left(q_{1JT}^2+q_{2JT}^2+q_{3JT}^2\right)\left(q_4^2+q_5^2+q_6^2\right)$$
$$+\lambda'_{qM2+R4+}\left(q_{1JT}^2q_4^2+q_{2JT}^2q_5^2+q_{3JT}^2q_6^2\right)$$
$$+\lambda_{qM2+M3+R4+}\left(q_{1JT}q_1q_5q_6+q_{2JT}q_2q_4q_6+q_{3JT}q_3q_4q_5\right). \quad (29)$$

For R_3^+ JT + tilting the equivalent terms are

$$\lambda_{qR3+M3+}\left(q_{4JT}^2+q_{5JT}^2\right)\left(q_1^2+q_2^2+q_3^2\right)+\lambda'_{qR3+M3+}$$
$$\left[q_{4JT}^2\left(q_1^2+\frac{q_2^2}{4}+\frac{q_3^2}{4}\right)+\frac{\sqrt{3}q_{4JT}q_{5JT}(q_2^2-q_3^2)}{2}+\frac{3q_{5JT}^2(q_2^2+q_3^2)}{4}\right]$$
$$+\lambda_{qR3+R4+}\left(q_{4JT}^2+q_{5JT}^2\right)\left(q_4^2+q_5^2+q_6^2\right)+\lambda'_{qR3+R4+}$$
$$\left[q_{4JT}^2\left(q_4^2+\frac{q_5^2}{4}+\frac{q_6^2}{4}\right)+\frac{\sqrt{3}q_{4JT}q_{5JT}\left(q_5^2-q_6^2\right)}{2}+\frac{3q_{5JT}^2\left(q_5^2+q_6^2\right)}{4}\right]. \quad (30)$$

When considering mixed JT + tilt systems, it is necessary to use twin components of each with the correct orientation relationships. The relevant unit-cell orientations, chosen to maintain the orientations of tilt axes from the purely tilted structures, are shown in Fig. 2 for the specific cases of *Imma* and *C*2/*m* ($\Gamma_3^+ + R_4^+$), *Pnma* ($M_2^+ + R_4^+ + M_3^+$) and the $P2_1/a$ setting of $P2_1/c$ ($R_3^+ + R_4^+ + M_3^+$). These are the most immediately pertinent settings in relation to known phases. Note that in the $M_2^+ + R_4^+ + M_3^+$ (*Pnma*) structure the M_2^+ twin component has order-parameter components (0, q_{2JT}, 0). In the absence of tilting the tetragonal axis of this twin component (which is perpendicular to the planes of ordered octahedra) would be aligned parallel to *X*. (q_{1JT}, 0, 0) and (0, 0, q_{3JT}) represent twinned variants with tetragonal axes parallel to *Z* and *Y*, respectively.

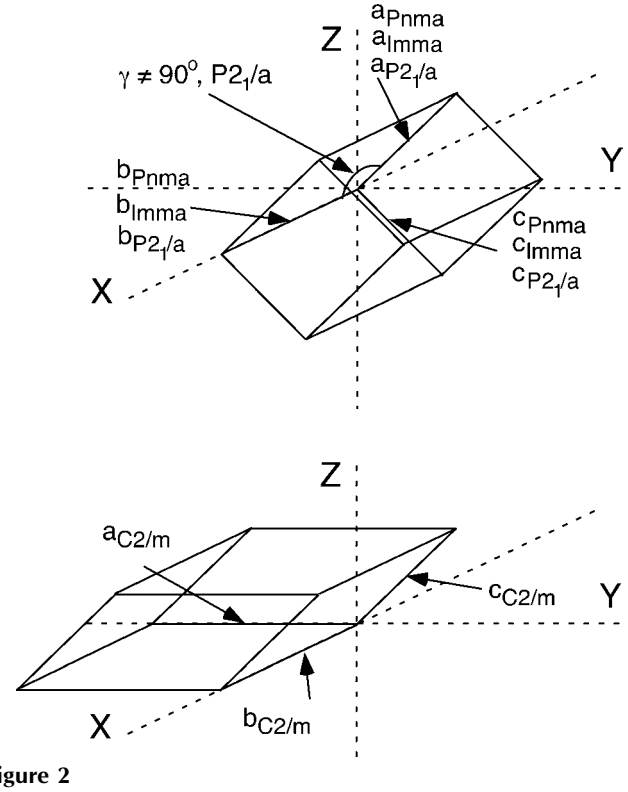

Figure 2
Unit-cell orientations with respect to the orthogonal reference system used to calculate strains in the case of structures with both Jahn–Teller distortions and octahedral tilting, and space groups *Imma*, *C*2/*m* ($\Gamma_3^+ + R_4^+$), *Pnma* ($M_2^+ + R_4^+ + M_3^+$), $P2_1/a$ setting of $P2_1/c$ ($R_3^+ + R_4^+ + M_3^+$).

For the R_3^+ pure JT structure (*I*4/*mcm*), the order-parameter components are (0, q_{5JT}) and orientational ordering of the octahedra occurs within the (001) plane. {As an aside, (q_{4JT}, 0) represents a different structure with *I*4/*mmm* symmetry, which has the unique axes of Q_3 octahedra all aligned parallel to [001]. Octahedra in alternating (001) layers would have different degrees of distortion, making this an unlikely JT structure.} The relevant R_3^+ contribution to the $P2_1/c$ structure ($P2_1/a$ setting) has JT order-parameter components of the form $\left(\frac{a\sqrt{3}}{2}, -\frac{a}{2}\right)$. This corresponds to a twin variant of the structure with $q_{5JT} \neq 0$, $q_{4JT} = 0$ in which the unique axis is aligned parallel to *X* (Fig. 2).

For a tilt plus Γ_3^+ JT structure with *Imma* or *Pnma* symmetry, the JT components have the form $\left(-\frac{a}{2}, -\frac{a\sqrt{3}}{2}\right)$. These could also be expressed as $q_{tx} \neq 0$, $q_{ox} = 0$ for a JT twin variant with the tetragonal axis parallel to *X*. With respect to strain orientations, it turns out to also be convenient to express the Γ_3^+ strains in terms of e_{tx} and e_{ox} where

$$e_{tx} = \frac{1}{\sqrt{3}}(2e_1 - e_2 - e_3) = -\frac{1}{2}\left(e_{tz} - \sqrt{3}e_{oz}\right) \quad (31)$$

and

$$e_{ox} = (e_2 - e_3) = -\frac{1}{2}\left(\sqrt{3}e_{tz} + e_{oz}\right). \quad (32)$$

4. Phase transitions

There is no *a priori* reason why tilting transitions should occur ahead of Jahn–Teller transitions, or *vice versa*, and sequences of the type cubic → tilt → tilt + JT and cubic → JT → tilt + JT can both occur. Table 2 summarizes the possibilities for tilting followed by Jahn–Teller ordering. If there is no change in symmetry, the JT transition is expected to be first order in character, in line with the general expectation for isosymmetric phase transitions (Christy, 1995). The $Pm\bar{3}m \leftrightarrow P4/mmm$ transition must be first order in character owing to the existence of third-order invariants of the order parameter in the excess free energy, but all the remaining transitions can be second order. Figs. 3, 4 and 5 show hierarchies of symmetry changes in which JT ordering (M_2^+, R_3^+ and Γ_3^+, respectively) precedes three separate phases of tilting. In these figures, the unique tetragonal axis of the pure JT structure has been set to be parallel to *Z* and the orientations of possible tilt axes allowed to differ from those of the equivalent pure tilted structures. Solid lines indicate transitions which are allowed by symmetry to be second order in character. Broken lines show transitions between related structures which are expected to be first order. In combination, Table 2 and Figs. 3–5 allow

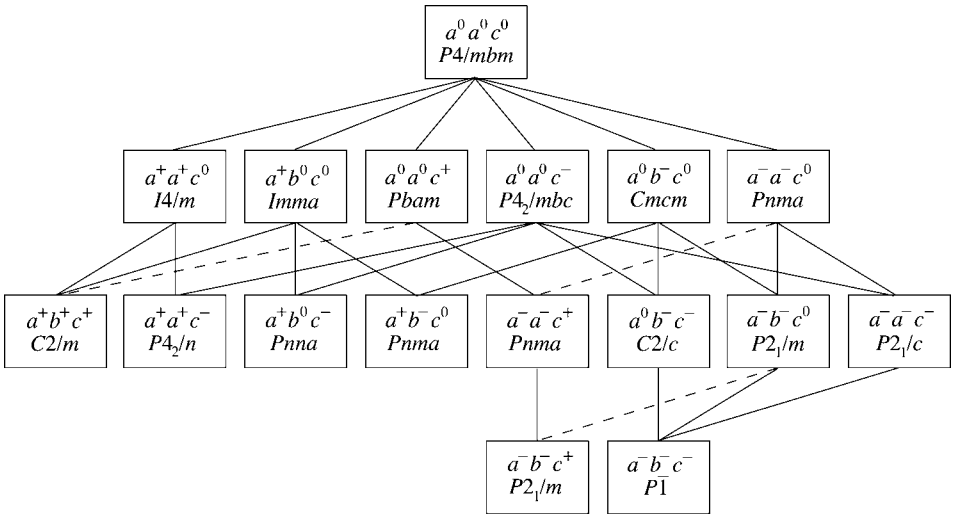

Figure 3
Symmetry hierarchy for tilting transitions in an ABX_3 perovskite with Jahn–Teller ordering corresponding to irrep M_2^+ and with the orientation of the JT ordered structure maintained. Solid lines indicate group–subgroup relationships for which transitions are allowed to be second order. Dashed lines indicate group–subgroup relationships for which transitions must be first order. Isosymmetric transitions are also shown as being first order.

more extensive transformation pathways, such as cubic → tilt → tilt + JT → additional tilt + JT, to be evaluated.

For M_2^+ and R_3^+ JT systems, coupling between a tilt order-parameter component, $q_{\rm tilt}$, and a JT order-parameter component, $q_{\rm JT}$, could either be direct or indirect *via* a common strain. With the exception of the term $\lambda_{\rm qM2+M3+R4+}(q_{1\rm JT}q_1q_5q_6 + q_{2\rm JT}q_2q_4q_6 + q_{3\rm JT}q_3q_4q_5)$, the coupling is effectively all of the form $\lambda q_{\rm tilt}^2 q_{\rm JT}^2$. Salje & Devarajan (1986) have investigated biquadratic coupling between two order parameters systematically and their results provide a qualitative picture of general possibilities for structural sequences with falling temperature. For compatible combinations of tilting and JT ordering, and second-order transitions, the tilting may precede or follow the ordering, as shown in Figs. 6(*a*) and (*b*), respectively. It is not necessarily the case that the coupling is favourable, however, and in the event that one process induces macroscopic strains which are opposite in sign to those associated with the other, the structure could revert back to a purely tilted or JT ordered form (Figs. 6*c* and *d*). In addition to the strength of coupling, the difference in critical temperatures between the tilt and JT instabilities plays a role in determining the extent to which the evolution of one order parameter modifies the evolution of the other. In general, the strongest influence is seen when the critical temperatures are similar. If they are widely separated, one order parameter will display only small deviations through the second transition (dashed lines in Figs. 6*a* and *b*). There can also be circumstances in which a mixed tilt + JT structure does not have any field of stability, so that the pure tilted structure transforms to the pure JT structure or *vice versa* (Figs. 6*e* and *f*). Coupling determined by $\lambda_{\rm qM2+M3+R4+}(q_{1\rm JT}q_1q_5q_6 + q_{2\rm JT}q_2q_4q_6 +$

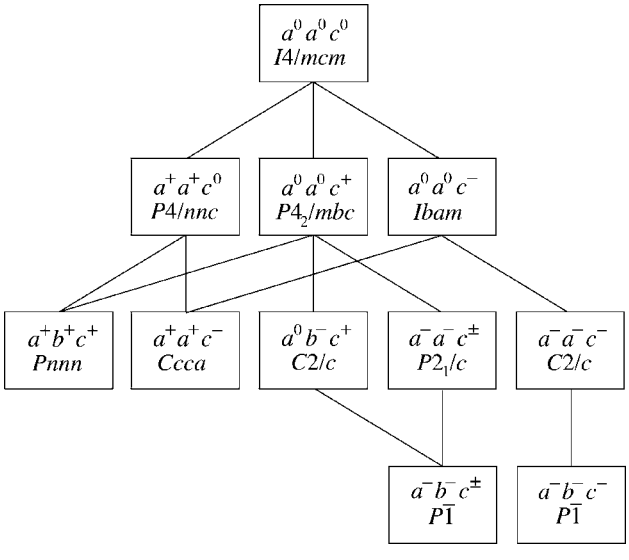

Figure 4
Symmetry hierarchy for tilting transitions in an ABX_3 perovskite with Jahn–Teller ordering corresponding to irrep R_3^+ and with the orientation of the JT ordered structure maintained. Solid lines indicate group–subgroup relationships for which transitions are allowed to be second order.

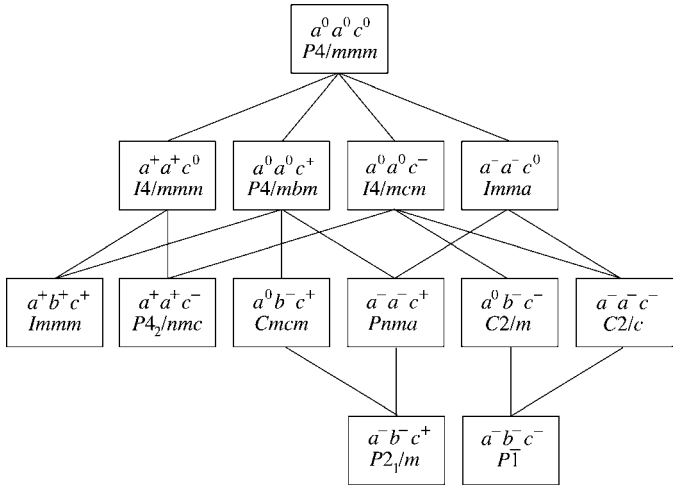

Figure 5
Symmetry hierarchy for tilting transitions in an ABX_3 perovskite with Jahn–Teller ordering corresponding to irrep Γ_3^+ and with the orientation of the JT ordered structure maintained. Solid lines indicate group–subgroup relationships for which transitions are allowed to be second order.

Table 3
Possible space groups for structures with combinations of Jahn–Teller ordering related to irreps $M_2^+ + R_3^+$.

Space group	M_2^+ $q_{1JT}q_{2JT}q_{3JT}$	R_3^+ $q_{4JT}q_{5JT}$	Lattice vectors	Origin
127 *P*4/*mbm*	(*a*,0,0)	(0,*b*)	(1,1,0)($\bar{1}$,1,0)(0,0,2)	($\frac{1}{2},\frac{1}{2}$,0)
131 $P4_2/mmc$	(0,*a*,*a*)	(0,*b*)	(2,0,0)(0,2,0)(0,0,2)	(0,0,0)
136 $P4_2/mnm$	(*a*,0,0)	(*b*,0)	(1,1,0)($\bar{1}$,1,0)(0,0,2)	(0,0,0)
123 *P*4/*mmm*	(0,*a*,*a*)	(*b*,0)	(2,0,0)(0,2,0)(0,0,2)	(1,0,0)
65 *Cmmm*	(*a*,0,0)	(*b*,*c*)	(2,0,0)(0,2,0)(0,0,2)	(0,0,0)
47 *Pmmm*	(*a*,*b*,*c*)	(*d*,*e*)	(2,0,0)(0,2,0)(0,0,2)	(0,0,0)

$q_{3JT}q_3q_4q_5$) could result in q_{JT} acting as a linear field for tilting, or in the tilting providing an effective field for JT ordering.

Coupling between Γ_3^+ orbital ordering and the tilt systems is slightly different in that linear-quadratic coupling terms of the form $\lambda q_{JT}q_{tilt}^2$ are permitted by symmetry (Carpenter *et al.*, 2005). Salje & Devarajan (1986) did not consider this case, but the same general principle must apply, namely that different sequences of phase transitions can occur, depending largely on the critical temperature for each of the two instabilities and the strength of coupling between them. As explained by Carpenter *et al.* (2005) for the case of $PrAlO_3$, one consequence of the linear-quadratic coupling is that the JT ordering can act as an applied field for the tilting, and *vice versa*.

In principle it is also possible to have mixed structures containing some degree of both M_2^+ and R_3^+ JT order. These have been derived from *ISOTROPY* (in the absence of tilting) and are listed in Table 3. They are also shown as a symmetry hierarchy in Fig. 7. The simplest mixed structure would have *P*4/*mbm* symmetry, and might occur, for example, if there was a crossover in stability between M_2^+ and R_3^+ structures as a function of temperature, pressure or composition. Coupling between the two different sets of JT order-parameter components would again be biquadratic, and the various sequences shown in Fig. 6 could all apply.

4.1. Structures in which tilting transitions occur prior to cooperative Jahn–Teller ordering

For most Jahn–Teller ions in perovskites, the energy changes associated with cooperative distortions are smaller than are associated with tilting, so that the tilting occurs at higher temperatures than the ordering. Thus, RVO_3 perovskites, where R = Yb, Ho, Y, Tb, ..., typically have the space group *Pnma* ($M_3^+ + R_4^+$) at room temperature, with the symmetry reduction from cubic being due to octahedral tilting alone (Miyasaka *et al.*, 2003; Sage *et al.*, 2007; Martínez-Lope *et al.*, 2008). At lower temperatures, they undergo a Jahn–Teller

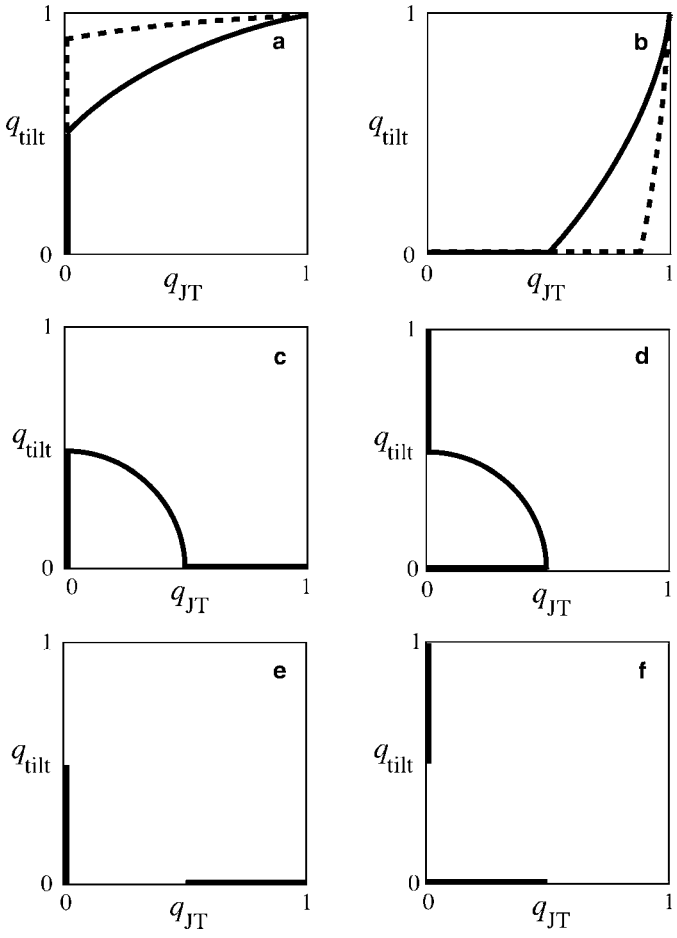

Figure 6
A selection of possible solutions from Salje & Devarajan (1986) for biquadratically coupled order parameters, $\lambda q_{tilt}^2 q_{JT}^2$, where q_{tilt} represents tilting and q_{JT} represents JT order. In (*a*), (*c*) and (*e*) the tilting instability occurs at a higher temperature than the JT instability. The reverse applies in (*b*), (*d*) and (*f*). The dashed lines in (*a*) and (*b*) indicate the form of order-parameter variations expected when the critical temperatures for the JT ordering and tilting are widely separated.

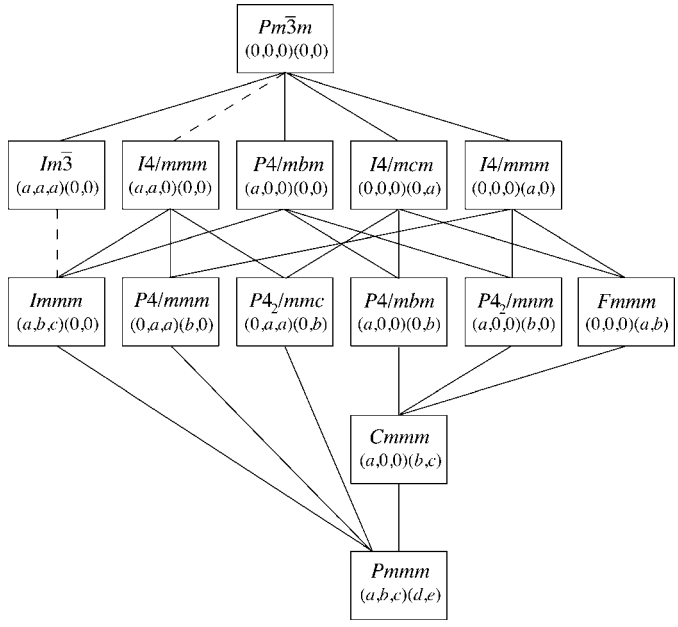

Figure 7
Symmetry hierarchy for 'pure' (*i.e.* without octahedral tilting) Jahn–Teller ordering transitions associated with combinations of irreps M_2^+ and R_3^+ in an ABX_3 perovskite. Solid lines indicate group–subgroup relationships for which transitions are allowed to be second order. Dashed lines indicate group–subgroup relationships for which transitions must be first order. Non-zero order-parameter components for each of the possible space groups are given in brackets.

orbital ordering transition, giving the symmetry change *Pnma* $\rightarrow$ $P2_1/c$ ($R_3^+ + M_3^+ + R_4^+$). Different space groups have been used to describe the monoclinic structure (*e.g.* Blake *et al.*, 2001, 2002; Bordet *et al.*, 1993; Muñoz *et al.*, 2003*a*,*b*, 2004*a*,*b*; Ren *et al.*, 2003; Reehuis *et al.*, 2006, Sage *et al.*, 2007), but the present symmetry analysis confirms $P2_1/c$ ($2a_p \times \sqrt{2}a_p \times \sqrt{2}a_p$) as being correct (Table 1). If it is desirable to keep the same unit cell as the *Pnma* structure, the non-standard setting is $P2_1/a$ ($\sqrt{2}a_p \times 2a_p \times \sqrt{2}a_p$) with γ as the monoclinic angle (Bordet *et al.*, 1993). If the chosen orthorhombic setting is *Pbnm*, the corresponding monoclinic setting is $P2_1/b$ ($\sqrt{2}a_p \times \sqrt{2}a_p \times 2a_p$), with α as the monoclinic angle (Ren *et al.*, 2003; Reehuis *et al.*, 2006; Sage *et al.*, 2007; Martínez-Lope *et al.*, 2008). Some vanadate perovskites undergo a further transition, $P2_1/c \rightarrow$ *Pnma* ($M_2^+ + M_3^+ + R_4^+$), in which the ordering scheme changes from R_3^+ (*a*-type) to M_2^+ (*d*-type). Summaries of this overall behaviour are given by Miyasaka *et al.* (2003) and Sage *et al.* (2007).

The Jahn–Teller ordered structure of $LaMnO_3$ also develops by octahedral tilting before undergoing Jahn–Teller ordering (Norby *et al.*, 1995; Rodríguez-Carvajal *et al.*, 1998; Mandal *et al.*, 2001; Mandal & Ghosh, 2003; Sánchez *et al.*, 2003; Chatterji *et al.*, 2003, 2004, 2006; Qiu *et al.*, 2005). In this case both the tilted structure ($M_3^+ + R_4^+$) and the Jahn–Teller structure ($M_2^+ + M_3^+ + R_4^+$) have the space group *Pnma*, and there is no symmetry change. A monoclinic phase with space group $P2_1/a$ and unit cell $\sqrt{2}a_p \times 2a_p \times \sqrt{2}a_p$, $\gamma \neq 90^\circ$ reported by Huang *et al.* (1997) has the same lattice geometry as the vanadate phase with R_3^+ Jahn–Teller distortions, but could also develop from the *Pnma* structure by the addition of a further R_4^+ tilt. Another monoclinic structure, stabilized by low oxygen fugacity, has been reported by Mitchell *et al.* (1996) as having the space group $P2_1/a$ and the unit cell $2a_p \times 2a_p \times 2a_p$. This does not appear in Table 1, however, and Rodríguez-Carvajal *et al.* (1998) showed that it can also be described under the space group *Pnma*. Although they have not been investigated extensively, the behaviour of $R\mathrm{MnO_3}$ phases would be expected to be broadly similar to that of $LaMnO_3$, at least in terms of the relative transition temperatures for octahedral tilting and Jahn–Teller ordering. At room temperature they have *Pnma* symmetry (Alonso *et al.*, 2000; Zhou & Goodenough, 2006; Tachibana *et al.*, 2007).

Perovskites in which the pattern of Jahn–Teller distortions conforms to Γ_3^+ as the active representation are relatively rare in comparison with those for which the active representation is M_2^+ or R_3^+. A prominent example is $PrAlO_3$ (Burbank, 1970; Kjems *et al.*, 1973; Birgeneau *et al.*, 1974; Cohen *et al.*, 1974; Sturge *et al.*, 1975; Lyons *et al.*, 1975; Harley *et al.*, 1973; Fujii *et al.*, 1999; Carpenter *et al.*, 2005; Watanabe *et al.*, 2006). The Jahn–Teller cation is on the crystallographic *A* site rather than the *B* site but, from a symmetry perspective, this difference is not important and the symmetry rules for coupling still apply. Recent powder neutron-diffraction studies suggest that the full transition sequence in $PrAlO_3$ is $Pm\bar{3}m \leftrightarrow R\bar{3}c \leftrightarrow$ *Imma* $\leftrightarrow C2/m$ (Moussa *et al.*, 2001; Howard *et al.*, 2000; Carpenter *et al.*, 2005). The $R\bar{3}c$ structure belongs to R_4^+ (pure tilt), while both the *Imma* and $C2/m$ structures belong to $\Gamma_3^+ + R_4^+$. The tendency for this structure is to evolve towards $I4/mcm$ (also $\Gamma_3^+ + R_4^+$) at the lowest temperatures, although tetragonal lattice geometry is not quite achieved (Carpenter *et al.*, 2005).

4.2. Structures in which Jahn–Teller transitions occur prior to octahedral tilting

Perovskites containing Cu^{2+} or Cr^{2+} on the octahedral site display cooperative Jahn–Teller distortions to the highest temperatures and are therefore the most likely to show octahedral tilting transitions in an already distorted structure. $KCuF_3$ can be grown with $I4/mcm$ (R_3^+) or $P4/mbm$ (M_2^+) Jahn–Teller structures, but the large *A*-site cation inhibits octahedral tilting. $RbCuF_3$ can be crystallized with the $I4/mcm$ structure, which is also maintained to at least room temperature (Kaiser *et al.*, 1990). On the other hand, $NaCuF_3$ has both JT distortions (R_3^+) and additional displacements at room temperature which Kaiser *et al.* (1990) referred to as deriving from the $GdFeO_3$ structure (*Pnma*, with M_3^+ and R_4^+ tilting). They proposed a triclinic space group, $P\bar{1}$. From Tables 1 and 2, it is apparent that $P\bar{1}$ is a possibility in terms of the group-theoretical analysis presented here, but so is $P2_1/c$. Whichever is the case, there may be a hierarchy of displacive transitions worthy of investigation at high temperatures, with the Jahn–Teller ordering scheme remaining essentially unchanged.

Evidence for a hierarchy of transitions has been found in $KCrF_3$ (Margadonna & Karotsis, 2006). The parent Jahn–Teller structure again has $I4/mcm$ (R_3^+) symmetry, and this disorders to the $Pm\bar{3}m$ structure *via* a strongly first-order transition at ~ 973 K (Margadonna & Karotsis, 2006, 2007). On cooling, the pure Jahn–Teller structure undergoes a tilting transition between 250 and 200 K to a structure which Margadonna & Karotsis (2006) assigned to the space group $I2/m$ and unit cell $\sqrt{2}a_p \times \sqrt{2}a_p \times 2a_p$, $\gamma \neq 90^\circ$. This is a different choice of unit cell for the $C2/m$ structure with unit cell $2a_p \times 2a_p \times \sqrt{2}a_p$, $\beta \neq 90^\circ$, which appears in Table 1. It does not appear in the list of possible structures with R_3^+ JT order, however. Either the ordering scheme changes with the tilting or the space group is incorrectly determined. An alternative monoclinic structure with R_3^+ order and $\sqrt{2}a_p \times \sqrt{2}a_p \times 2a_p$ unit cell might be the $I2/a$ setting of $C2/c$. Below 30 K there is another apparently first-order transition to a structure which Margadonna & Karotsis again assigned to $I2/m$. From the perspective of the group-theoretical analysis, there are several possibilities, but a sequence $Pm\bar{3}m \rightarrow I4/mcm$ (R_3^+ only) $\rightarrow C2/c$ ($R_3^+ + R_4^+$) $\rightarrow C2/c$ or $P2_1/c$ ($R_3^+ + M_3^+ + R_4^+$) would be worth considering in any reanalysis of diffraction data for $KCrF_3$.

A rare example of a Γ_3^+ Jahn–Teller system without octahedral tilting appears to be $La_{0.5}Ba_{0.5}CoO_3$ (Fauth *et al.*, 2001; Nakajima *et al.*, 2005). The form with a disordered distribution of La and Ba on the crystallographic *A* sites undergoes a $Pm\bar{3}m \leftrightarrow P4/mmm$ transition which has been ascribed to cooperative Jahn–Teller distortions of the CoO_6 octahedra, favoured by at least some of the Co^{3+} and Co^{4+} ions having intermediate spin states (Fauth *et al.*, 2001; Nakajima *et al.*, 2005).

5. Cation ordering

Ordering of cations, *e.g.* distinct cations on the *A* sites of $LaBaCo_2O_6$ (Nakajima *et al.*, 2005; Kundu *et al.*, 2007; Rautama *et al.*, 2008) and on the *B* sites of Ba_2CuWO_6 (Iwanaga *et al.*, 1999) or Mn with different charge on the *B* sites of $NdSrMn_2O_6$ (Woodward *et al.*, 1999), provides an additional structural variable which will influence both Jahn–Teller distortions and octahedral tilting, with knock-on consequences for electrical and magnetic properties. Possible *B*-site ordered structures and the effect of cation ordering on cooperative JT distortion schemes have been discussed in detail by Lufaso & Woodward (2004), who described three distinct ordering arrangements. From the perspective adopted in the present study, the addition of such ordering can be described by the introduction of a further order parameter. Ordering on the basis of the rocksalt structure changes the space-group symmetry from $Pm\overline{3}m$ to $Fm\overline{3}m$, with unit cell $2a_p \times 2a_p \times 2a_p$. In this case the order parameter belongs to R_1^+ (Howard *et al.*, 2003). An alternative ordering scheme has the different cations alternating in layers which, in the absence of tilting or JT distortions, would give *P*4/*mmm* symmetry and unit cell $a_p \times a_p \times 2a_p$. In this case the active representation is X_3^- (Howard & Zhang, 2004*a*,*b*). A third scheme has *B*-site cations ordered in alternating chains such that, in the absence of Jahn–Teller distortions and octahedral tilting, the space group would become *P*4/*mmm* with a $\sqrt{2}a_p \times \sqrt{2}a_p \times a_p$ unit cell. In this case the active representation is M_1^+. Different combinations of order parameters belonging to these representations with order parameters for cooperative Jahn–Teller distortions and octahedral tilting lead to three further hierarchies of structures analogous to those shown in Table 1. The hierarchy of tilted structures in a starting material with the $a_p \times a_p \times 2a_p$, *P*4/*mmm* ordering scheme has already been determined by Howard & Zhang (2004*a*,*b*). The remaining two will be presented elsewhere.

6. Conclusion

The new symmetry hierarchies presented here for different combinations of octahedral tilting and cooperative Jahn–Teller ordering provide a template against which proposed structure types for complex perovskites containing Jahn–Teller ions can be tested. A comprehensive survey of all reported structures has not been attempted but it appears that, from even a brief review of selected monoclinic structures, some appear in Table 1 while others do not. It is anticipated that new variants will be discovered as the range of multi-component solid solutions is extended in the search for materials with better or different electronic properties. More importantly, perhaps, is the recognition that coupling processes in these materials can be determined by strain relaxations in exactly the same manner as in other ferroelastic perovskites. Expressions for the formal strain/order-parameter relationships will allow the use of symmetry-adapted strains, from high-resolution lattice-parameter data alone, to investigate the strength of coupling and the dependence of each order parameter on temperature, pressure and composition.

Support from the Leverhulme Trust, in the form of a Visiting Professorship for CJH, and from the Australian Research Council (grant No. DP0877695) is gratefully acknowledged.

References

Ahn, K. H., Lookman, T. & Bishop, A. R. (2004). *Nature*, **428**, 401–404.
Ahn, K. H., Lookman, T., Saxena, A. & Bishop, A. R. (2005). *Phys. Rev. B*, **71**, 212102.
Ahn, K. H. & Millis, A. J. (2001). *Phys. Rev. B*, **64**, 115103.
Alonso, J. A., Martínez-Lope, M. J., Casais, M. T. & Fernández-Díaz, M. T. (2000). *Inorg. Chem.* **39**, 917–923.
Birgeneau, R. J., Kjems, J. K., Shirane, G. & Van Uitert, L. G. (1974). *Phys. Rev. B*, **10**, 2512–2534.
Blake, G. R., Palstra, T. T. M., Ren, Y., Nugroho, A. A. & Menovsky, A. A. (2001). *Phys. Rev. Lett.* **87**, 245501.
Blake, G. R., Palstra, T. T. M., Ren, Y., Nugroho, A. A. & Menovsky, A. A. (2002). *Phys. Rev. B*, **65**, 174112.
Bock, O. & Müller, U. (2002). *Acta Cryst.* B**58**, 594–606.
Bordet, P., Chaillout, C., Marezio, M., Huang, Q., Santoro, A., Cheong, S.-W., Takagi, H., Oglesby, C. S. & Batlogg, B. (1993). *J. Solid State Chem.* **106**, 253–270.
Burbank, R. D. (1970). *J. Appl. Cryst.* **3**, 112–120.
Burgy, J., Moreo, A. & Dagotto, E. (2004). *Phys. Rev. Lett.* **92**, 097202.
Calderón, M. J., Millis, A. J. & Ahn, K. H. (2003). *Phys. Rev. B*, **68**, 100401.
Carpenter, M. A. (2007). *Am. Mineral.* **92**, 309–327.
Carpenter, M. A., Becerro, A. I. & Seifert, F. (2001). *Am. Mineral.* **86**, 348–363.
Carpenter, M. A., Boffa Ballaran, T. & Atkinson, A. J. (1999). *Phase Transitions*, **69**, 95–109.
Carpenter, M. A. & Howard, C. J. (2009). *Acta Cryst.* B**65**, 147–159.
Carpenter, M. A., Howard, C. J., Kennedy, B. J. & Knight, K. S. (2005). *Phys. Rev. B*, **72**, 024118.
Chapman, J. P., Attfield, J. P., Rodriguez-Martinez, L. M., Lezama, L. & Rojo, T. (2004). *Dalton Trans.* pp. 3026–3031.
Chatterji, T., Fauth, F., Ouladdiaf, B., Mandal, P. & Ghosh, B. (2003). *Phys. Rev. B*, **68**, 052406.
Chatterji, T., Ouladdiaf, B., Mandal, P. & Ghosh, B. (2004). *Solid State Commun.* **131**, 75–80.
Chatterji, T., Riley, D., Fauth, F., Mandal, P. & Ghosh, B. (2006). *Phys. Rev. B*, **73**, 094444.
Christy, A. G. (1995). *Acta Cryst.* B**51**, 753–757.
Cohen, E., Sturge, M. D., Birgeneau, R. J., Blount, E. I. & Van Uitert, L. G. (1974). *Phys. Rev. Lett.* **32**, 232–235.
Cox, S., Loudon, J. C., Williams, A. J., Attfield, J. P., Singleton, J., Midgley, P. A. & Mathur, N. D. (2008). *Phys. Rev. B*, **78**, 035129.
Fauth, F., Suard, E. & Caignaert, V. (2001). *Phys. Rev. B*, **65**, 060401.
Fujii, H., Hidaka, M. & Wanklyn, B. M. (1999). *Phase Transitions*, **70**, 115–132.
Glazer, A. M. (1972). *Acta Cryst.* B**28**, 3384–3392.
Goodenough, J. B. (1998). *Ann. Rev. Mater. Sci.* **28**, 1–27.
Goodenough, J. B. (2004). *Rep. Prog. Phys.* **67**, 1915–1993.
Gu, R. Y. & Ting, C. S. (2002). *Phys. Rev. B*, **65**, 214426.
Harley, R. T., Hayes, W., Perry, A. M. & Smith, S. R. P. (1973). *J. Phys. C*, **6**, 2382–2400.
Hemberger, J., Krug von Nidda, H.-A., Fritsch, V., Deisenhofer, J., Lobina, S., Rudolf, T., Lunkenheimer, P., Lichtenberg, F., Loidl, A., Bruns, D. & Büchner, B. (2003). *Phys. Rev. Lett.* **91**, 066403.
Horsch, P., Oles, A. M., Feiner, L. F. & Khaliullin, G. (2008). *Phys. Rev. Lett.* **100**, 167205.

Howard, C. J., Kennedy, B. J. & Chakoumakos, B. C. (2000). *J. Phys. Condens. Matter*, **12**, 349–365.
Howard, C. J., Kennedy, B. J. & Woodward, P. M. (2003). *Acta Cryst.* B**59**, 463–471.
Howard, C. J. & Stokes, H. T. (1998). *Acta Cryst.* B**54**, 782–789.
Howard, C. J. & Stokes, H. T. (2004). *Acta Cryst.* B**60**, 674–684.
Howard, C. J. & Stokes, H. T. (2005). *Acta Cryst.* A**61**, 93–111.
Howard, C. J. & Zhang, Z. (2004*a*). *Acta Cryst.* B**60**, 249–251.
Howard, C. J. & Zhang, Z. (2004*b*). *Acta Cryst.* B**60**, 763.
Huang, Q., Santoro, A., Lynn, J. W., Erwin, R. W., Borchers, J. A., Peng, J. L. & Greene, R. L. (1997). *Phys. Rev. B*, **55**, 14987–14999.
Israel, C., Calderón, M. J. & Mathur, N. D. (2007). *Nat. Mater.* **10**, 24–32.
Iwanaga, D., Inaguma, Y. & Itoh, M. (1999). *J. Solid State Chem.* **147**, 291–295.
Kaiser, V., Otto, M., Binder, K. & Babel, D. (1990). *Z. Anorg. Allg. Chem.* **585**, 93–104.
Kjems, J. K., Shirane, G., Birgeneau, R. J. & Van Uitert, L. G. (1973). *Phys. Rev. Lett.* **31**, 1300–1303.
Komarek, A. C., Roth, H., Cwik, M., Stein, W.-D., Baier, J., Kriener, M., Bourée, F., Lorenz, T. & Braden, M. (2007). *Phys. Rev. B*, **75**, 224402.
Kundu, A. K., Rautama, E.-L., Boullay, Ph., Caignaert, V., Pralong, V. & Raveau, B. (2007). *Phys. Rev. B*, **76**, 184432.
Lufaso, M. W. & Woodward, P. M. (2004). *Acta Cryst.* B**60**, 10–20.
Lyons, K. B., Birgeneau, R. J., Blount, E. I. & Van Uitert, L. G. (1975). *Phys. Rev. B*, **11**, 891–900.
Mandal, P., Bandyopadhyay, B. & Ghosh, B. (2001). *Phys. Rev. B*, **64**, 180405.
Mandal, P. & Ghosh, B. (2003). *Phys. Rev. B*, **68**, 014422.
Margadonna, S. & Karotsis, G. (2006). *J. Am. Chem. Soc.* **128**, 16436–16437.
Margadonna, S. & Karotsis, G. (2007). *J. Mater. Chem.* **17**, 2013–2020.
Martínez-Lope, M. J., Alonso, J. A., Retuerto, M. & Fernández-Díaz, M. T. (2008). *Inorg. Chem.* **47**, 2634–2640.
Millis, A. J. (1998). *Nature*, **392**, 147–150.
Millis, A. J., Darling, T. & Migliori, A. (1998). *J. Appl. Phys.* **83**, 1588–1591.
Mitchell, J. F., Argyriou, D. N., Potter, C. D., Hinks, D. G., Jorgensen, J. D. & Bader, S. D. (1996). *Phys. Rev. B*, **54**, 6172–6183.
Miyasaka, S., Okimoto, Y., Iwama, M. & Tokura, Y. (2003). *Phys. Rev. B*, **68**, 100406.
Mizokawa, T., Khomskii, D. I. & Sawatzky, G. A. (1999). *Phys. Rev. B*, **60**, 7309–7313.
Moussa, S. M., Kennedy, B. J., Hunter, B. A., Howard, C. J. & Vogt, T. (2001). *J. Phys. Condens. Matter*, **13**, L203–L209.
Muñoz, A., Alonso, J. A., Casais, M. T., Martínez-Lope, M. J., Martínez, J. L. & Fernández-Díaz, M. T. (2003*a*). *J. Mater. Chem.* **13**, 1234–1240.
Muñoz, A., Alonso, J. A., Casáis, M. T., Martínez-Lope, M. J., Martínez, J. L. & Fernández-Díaz, M. T. (2003*b*). *Phys. Rev. B*, **68**, 144429.
Muñoz, A., Alonso, J. A., Casais, M. T., Martínez-Lope, M. J., Martínez, J. L. & Fernández-Díaz, M. T. (2004*a*). *Chem. Mater.* **16**, 1544–1550.
Muñoz, A., Alonso, J. A., Casais, M. T., Martínez-Lope, M. J., Martínez, J. L. & Fernández-Díaz, M. T. (2004*b*). *J. Magn. Magn. Mater.* **272–276**, 2163–2164.
Nakajima, T., Ichihara, M. & Ueda, Y. (2005). *J. Phys. Soc. Jpn*, **74**, 1572–1577.
Norby, P., Krogh Andersen, I. G., Krogh Andersen, E. & Andersen, N. H. (1995). *J. Solid State. Chem.* **119**, 191–196.
Okazaki, A. (1969*a*). *J. Phys. Soc. Jpn*, **26**, 870.
Okazaki, A. (1969*b*). *J. Phys. Soc. Jpn*, **27**, 518B.
Podzorov, V., Kim, B. G., Kiryukhin, V., Gershenson, M. E. & Cheong, S.-W. (2001). *Phys. Rev. B*, **64**, 140406.
Qiu, X., Proffen, Th., Mitchell, J. F. & Billinge, S. J. L. (2005). *Phys. Rev. Lett.* **94**, 177203.
Rautama, E.-L., Boullay, P., Kundu, A. S., Caignaert, V., Pralong, V., Karppinen, M. & Raveau, B. (2008). *Chem. Mater.* **20**, 2742–2750.
Reehuis, M., Ulrich, C., Pattison, P., Ouladdiaf, B., Rheinstädter, M. C., Ohl, M., Regnault, L. P., Miyasaka, M., Tokura, Y. & Keimer, B. (2006). *Phys. Rev. B*, **73**, 094440.
Ren, Y., Nugroho, A. A., Menovsky, A. A., Strempfer, J., Rütt, U., Iga, F., Takabatake, T. & Kimball, C. W. (2003). *Phys. Rev. B*, **67**, 014107.
Rodríguez-Carvajal, J., Hennion, M., Moussa, F., Moudden, A. H., Pinsard, L. & Revcolevschi, A. (1998). *Phys. Rev. B*, **57**, R3189–R3192.
Sage, M. H., Blake, G. R., Marquina, C. & Palstra, T. T. M. (2007). *Phys. Rev. B*, **76**, 195102.
Salamon, M. B. & Jaime, M. (2001). *Rev. Mod. Phys.* **73**, 583–628.
Salje, E. K. H. & Devarajan, V. (1986). *Phase Transitions*, **6**, 235–248.
Sánchez, M. C., Subías, G., García, J. & Blasco, J. (2003). *Phys. Rev. Lett.* **90**, 045503.
Stokes, H. T., Hatch, D. M. & Campbell, B. J. (2007). *ISOTROPY*, http://stokes.byu.edu/isotropy.html.
Stokes, H. T., Kisi, E. H., Hatch, D. M. & Howard, C. J. (2002). *Acta Cryst.* B**58**, 934–938.
Sturge, M. D., Cohen, E., Van Uitert, L. G. & van Stapele, R. P. (1975). *Phys. Rev. B*, **11**, 4768–4779.
Tachibana, M., Shimoyama, T., Kawaji, H., Atake, T. & Takayama-Muromachi, E. (2007). *Phys. Rev. B*, **75**, 144425.
Tamazyan, R. & van Smaalen, S. (2007). *Acta Cryst.* B**63**, 190–200.
Uehara, M. & Cheong, S.-W. (2000). *Europhys. Lett.* **52**, 674–680.
Watanabe, S., Hidaka, M., Yoshizawa, H. & Wanklyn, B. M. (2006). *Phys. Status Solidi B*, **243**, 424–434.
Wollan, E. O. & Koehler, W. C. (1955). *Phys. Rev.* **100**, 545–563.
Woodward, P. M. (1997*a*). *Acta Cryst.* B**53**, 32–43.
Woodward, P. M. (1997*b*). *Acta Cryst.* B**53**, 44–66.
Woodward, P. M., Cox, D. E., Vogt, T., Rao, C. N. R. & Cheetham, A. K. (1999). *Chem. Mater.* **11**, 3528–3538.
Zhou, J.-S. & Goodenough, J. B. (2006). *Phys. Rev. Lett.* **96**, 247202.
Zhou, J.-S., Goodenough, J. B., Yan, J.-Q. & Ren, Y. (2007). *Phys. Rev. Lett.* **99**, 156401.